Title
A TEST OF THE AS=AQ RULE IN LEPTONIC DECAYS OP NEUTRAL K MESONS

Author
Webber, Bryan Ronald.

Publication Date
1969-05-10

UCRL-19226

eg. 2

A TEST OF THE $\Delta S = \Delta Q$ RULE IN LEPTONIC DECAYS OF NEUTRAL K MESONS

Bryan Ronald Webber
(Ph. D. Thesis)

May 10, 1969

AEC Contract No. W-7405-eng-48

LAWRENCE RADIATION LABORATORY
UNIVERSITY of CALIFORNIA BERKELEY

UCRL-19226

eg. 2

DISCLAIMER

A TEST OF THE $\Delta S=\Delta Q$ RULE

IN LEPTONIC DECAYS OF NEUTRAL K MESONS

Contents

A TEST OF THE $\Delta S = \Delta Q$ RULE IN LEPTONIC DECAYS OF NEUTRAL K MESONS

Bryan Ronald Webber

Lawrence Radiation Laboratory
University of California
Berkeley, California

May 10, 1969

ABSTRACT

In 1.3 million hydrogen bubble chamber pictures, taken during an exposure of the 25-inch Lawrence Radiation Laboratory chamber to a 400 MeV/c K^- beam, we have found about 18 000 reactions of the type $K^- p \to \overline{K}^0 n$ followed by a visible decay of the neutral K meson. After applying many selection criteria, we find 252 events in which the decay is leptonic or radiative: neutral $K \to \pi^{\pm} e^{\mp} \nu$, $\pi^{\pm} \mu^{\mp} \nu$, or $\pi^+ \pi^- \gamma$. We have identified an electron in 81 of these events, and a muon in 38 of them. The remaining 133 events are treated as completely ambiguous between the leptonic and radiative decay hypotheses. By studying the time distributions of the identified and the ambiguous events, we test the $\Delta S = \Delta Q$ selection rule and also the Sachs model of CP violation, which predicts a large CP-violating $\Delta S = -\Delta Q$ term in the leptonic decay amplitudes. We define parameters, x for the electronic decay distributions and x' for the muonic, that are real if CP is conserved in the leptonic decays and are zero if $\Delta S = \Delta Q$. From the identified events, we find $\mathrm{Re}(x) = 0.30^{+0.10}_{-0.12}$, $\mathrm{Im}(x) = 0.07^{+0.10}_{-0.08}$ and $\mathrm{Re}(x') = 0.19^{+0.13}_{-0.18}$, $\mathrm{Im}(x') = -0.12^{+0.20}_{-0.17}$. Since these results are consistent with the hypothesis $x=x'$, we make this assumption in order to parametrize the distribution of ambiguous events in terms of x, and combine the results for all 252 events, to obtain $\mathrm{Re}(x) = 0.25^{+0.07}_{-0.09}$, $\mathrm{Im}(x) =$

0.00 ± 0.08. The relative likelihood of the value $x=0$ is $e^{-3.2}$, so this value lies about 2.5 standard deviations from the most likely value, and to this extent our experiment indicates a violation of the $\Delta S = \Delta Q$ rule. We find no significant imaginary part of x, which makes the Sachs mechanism of CP violation appear unlikely, although this model may not be ruled out with certainty, since it makes only an order-of-magnitudeprediction of Im(x). In order to correct the distribution of the ambiguous events for the background of $\pi^+\pi^-\gamma$ decays, we have to assume that radiative decay occurs only through inner bremsstrahlung in the process $K_S \rightarrow \pi^+\pi^-$. A study of 10 kinematically unambiguous $\pi^+\pi^-\gamma$ decays gives experimental support to this assumption. As consistency checks on our data, we measure the leptonic decay rate of the K_L, $\Gamma_L(\ell)$, and the absolute value of the K_S-K_L mass difference, $|\delta|$. Assuming our most likely value of x, we find $\Gamma_L(\ell) = (11.5 \pm 1.1) \times 10^6$ sec^{-1} and $|\delta| = (0.56^{+0.09}_{-0.08}) \times 10^{10}$ sec^{-1}, in good agreement with the established values of these quantities.

I. INTRODUCTION

In 1958, Feynman and Gell-Mann[1] proposed an empirical rule for weak interactions which has become known as the "$\Delta S = \Delta Q$" rule. They considered a weak interaction Hamiltonian with a current-current form:

$$H_{weak} = J_\mu J^\dagger_\mu + J^\dagger_\mu J_\mu, \tag{1}$$

and split the current up into non-strange hadronic, strange hadronic, and leptonic parts:

$$J_\mu = N_\mu + S_\mu + L_\mu . \tag{2}$$

Then the rule is concerned only with the strange hadronic current S_μ, and states that the strangeness of this current is equal to its charge, which is equal to + 1. Thus the operators S_μ and $S^\dagger_\mu$ can only connect hadronic states whose strangeness and charge differ by the same amount; that is, $S_\mu(S^\dagger_\mu)$ induces $\Delta S = \Delta Q = +1$ (-1) transitions.

The rule was originally proposed to account for the observation of the cascade decay

$$\Xi^- \to \Lambda\pi^- \; ; \quad \Lambda \to n\pi^0 , \tag{3}$$

instead of the direct transition

$$\Xi^- \to n\pi^- , \tag{4}$$

for if there existed a current S'_μ with $S = -Q = -1$, then the term $S'^\dagger_\mu S_\mu$ would induce the transition (4), for example, via a Λ intermediate state:

$$\langle n\pi^- | S'^\dagger_\mu | \Lambda \rangle \langle \Lambda | S_\mu | \Xi^- \rangle \neq 0. \tag{5}$$

Study of the hadron currents in non-leptonic processes such as (4), however, is complicated by our ignorance of strong interaction dynamics.[26] This complication is greatly reduced in the leptonic decays of strange particles, where the relevant terms of H_{weak} are $S_\mu L^\dagger_\mu$ and

$S^{\dagger}_{\mu} L_{\mu}$, since the leptonic current is very well understood. Thus good quantitative tests of the $\Delta S = \Delta Q$ rule did not become possible until the acquisition of large numbers of strange particle leptonic decays. Table I shows the status of the rule in these processes, prior to our experiment.[2]

Table I. Tests of the $\Delta S = \Delta Q$ Rule.

Process	$\Delta S/\Delta Q$	$\lvert g_{S'}/g_S \rvert$	Current
$\Sigma^+ \to n\, \ell^+ \nu$	-1	< 0.20	V and A
$\Sigma^- \to n\, \ell^- \bar{\nu}$	+1		
$K^+ \to \pi^+ \pi^+ e^- \bar{\nu}$	-1	< 0.23	A
$K^+ \to \pi^+ \pi^- e^+ \nu$	+1		dominates
$K^o \to \pi^+ \ell^- \bar{\nu}$	-1	0.21 ± 0.07	pure V
$K^o \to \pi^- \ell^+ \nu$	+1		

In this table, ℓ represents a lepton (e or μ) and g_S and $g_{S'}$ are the coupling constants of the $\Delta S = \Delta Q$ current S_μ and the $\Delta S = -\Delta Q$ current S'_μ respectively. One may separate these currents into their vector and axial vector parts, and the last column of the table shows which part contributes in each process. Since the relationship between the vector and axial vector currents is not understood, a test applied to one of them provides no presently useful information about the other. The $K^o_{\ell 3}$ decays therefore provide the only test of the $\Delta S = \Delta Q$ rule for a pure vector current.[27]

Since 1963, when the Cabibbo theory[3] was introduced, the $\Delta S = \Delta Q$ rule has been a basic tenet of weak interaction theory. Cabibbo pro-

posed that the hadronic weak currents are the charged members of an octet representation of the higher symmetry group SU(3). Then the strange currents transform under SU(3) like K^+ and K^- mesons, and, in particular, they have $S=Q=\pm 1$. We see from the Gell-Mann-Nishijima formula

$$Q = I_3 + \tfrac{1}{2}S \ , \qquad (6)$$

where I_3 is the third component of the isospin, that a current with $S = -Q = \pm 1$, on the other hand, has $I_3 = \pm 3/2$, and cannot be a member of an octet. Thus a violation of the $\Delta S = \Delta Q$ rule would be evidence of currents belonging to other SU(3) multiplets. In view of this, suggestions by previous experiments[4] of a violation in the $K^0_{\ell 3}$ decays, as indicated in Table I, are of great interest. Our experiment was undertaken in order to shed more light on the validity of the rule in these decays.

We obtained $\overline{K}^0$ mesons by exposing the 25-inch Lawrence Radiation Laboratory hydrogen bubble chamber to a K^- beam with momenta in the range 310-430 MeV/c. In a total of 1.3 million pictures, we found about 18 000 reactions of the type $K^- p \to \overline{K}^0 n$ followed by a visible decay of the neutral K meson. Most of these are $\pi^+\pi^-$ decays, but we have found 252 events in which the decay is leptonic or radiative: neutral $K \to \pi^\pm e^\mp \nu$, $\pi^\pm \mu^\mp \nu$, or $\pi^+\pi^-\gamma$. In 119 of these events the decay is definitely leptonic, and we regard the remaining 133 as completely ambiguous between the leptonic and radiative decay hypotheses. Using these 252 events, we are able to test the $\Delta S = \Delta Q$ rule with an accuracy comparable to that of any previous individual experiment.[5] Our results may be interpreted as giving a value of $|g_S'/g_S|$ of $0.25^{+0.07}_{-0.09}$.

Although we do not regard this result as entirely conclusive evidence of a violation of the rule, it does provide strong support for previous indications of a violation.

A test of the $\Delta S = \Delta Q$ rule in the Σ leptonic or $K^+_{\ell 4}$ decays is conceptually simple: the branching ratio of the forbidden decay mode relative to the allowed one provides a measure of $|g_S' / g_S|^2$. In the $K^o_{\ell 3}$ decays the situation is quite different, because of the unique properties of neutral K mesons. The experimentally observed neutral K states do not have definite strangeness, but are approximately the eigenstates of CP:

$$|K_S\rangle = \frac{1}{2} \left(|K^o\rangle + |\overline{K}^o\rangle \right) \qquad (7)$$

$$|K_L\rangle = \frac{1}{2} \left(|K^o\rangle - |\overline{K}^o\rangle \right)$$

The K_S decays predominantly into two pions, and has a short lifetime (0.862×10^{-10} sec), while the K_L has mainly leptonic and three-pion decay modes, and a much longer lifetime (538×10^{-10} sec). We see as follows that the $\Delta S = \Delta Q$ rule operates not to forbid certain decays of these states, but rather to predict the time distributions of the leptonic decays.

Consider a neutral K state which is a pure $\overline{K}^o$ at proper time $t = 0$. After a few times 10^{-10} seconds, the K_S half of the state has decayed away, leaving the K_L half, which is itself one half $\overline{K}^o$. Thus the $\overline{K}^o$ intensity in the state falls from 100 % to 25 % as shown in Fig. 1. Similarly, the K^o intensity rises from zero to 25 % in a few times 10^{-10} seconds, as shown in Fig. 2. Now the $\Delta S = \Delta Q$ rule states that only the $K^o (\overline{K}^o)$ part of the state can decay into $(\pi^- \ell^+ \nu)$ $(\pi^+ \ell^- \nu)$. Consequently, Figs. 1 and 2 also show the predicted shapes and relative

normalization of the negative and positive leptonic decay time distributions, respectively.

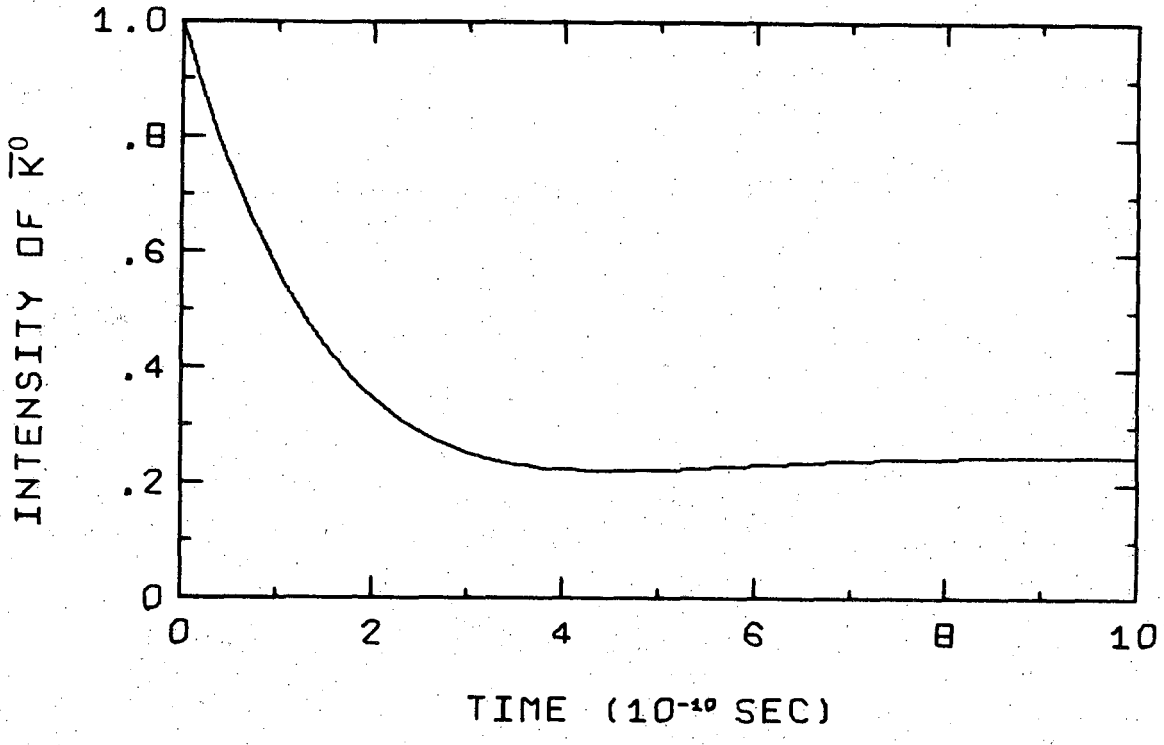

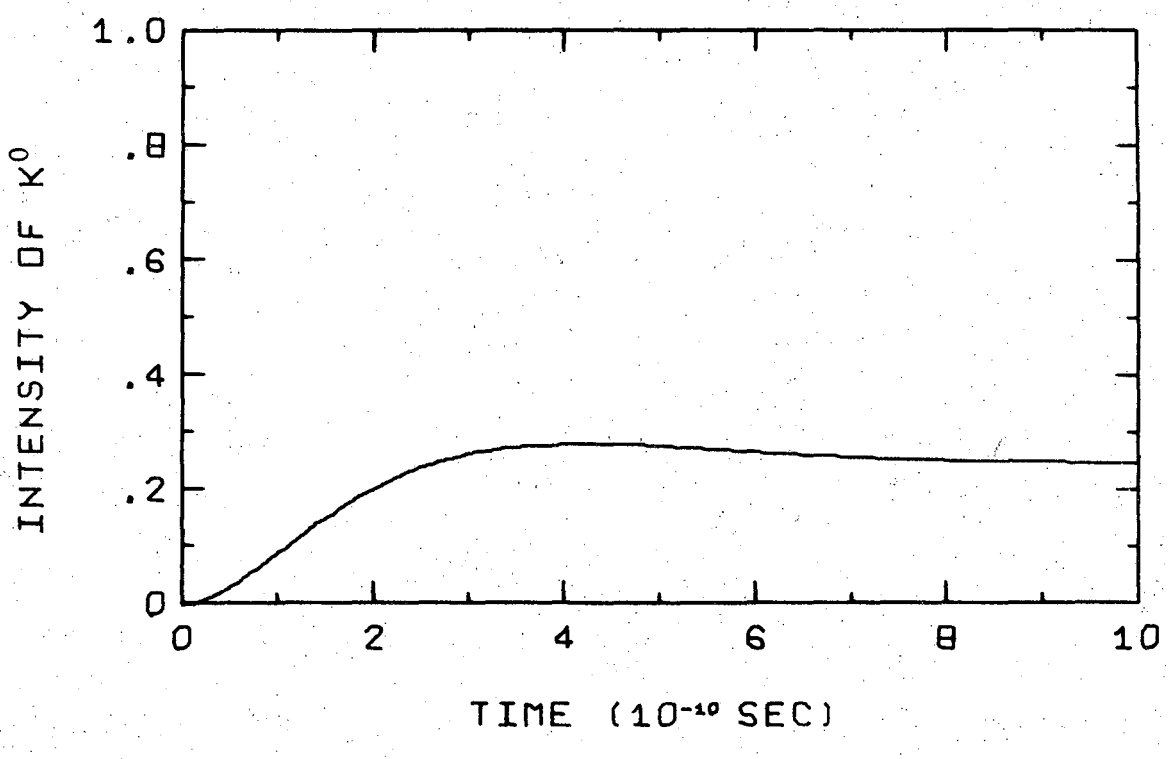

Figs. 1 and 2. Evolution of a state that is initially a $\overline{K}^0$.

If the $\Delta S = \Delta Q$ rule is violated, the time distributions will be different from those shown in Figs. 1 and 2. In Section II we discuss the distributions quantitatively, and show that they can be described in terms of two complex parameters, x for the electronic and x' for the muonic decays, which represent average values of the coupling ratio $g_{S'}/g_S$. The rule therefore predicts that x and x' are zero.

Since the time distributions are sensitive to the relative phase of the $\Delta S/\Delta Q = +1$ and -1 couplings, we can also test a model of CP violation proposed by Sachs.[6] In this model, which is discussed in detail in Appendix A, the observed CP-violating decays $K_L \to \pi^+\pi^-$ and $K_L \to \pi^o\pi^o$ take place owing to a gross violation of CP in the leptonic neutral K decays. We show in Section II that this would mean that x and x' have significant imaginary parts. We see no evidence of such imaginary parts in our experiment, so our results do not support the Sachs model. However, we are not able to rule out this model with certainty, because it makes only order-of-magnitude predictions of Im(x) and Im(x').

II. THEORY

A. General Form of the Time Distributions

In this section we derive the leptonic decay time distributions, without any special assumptions about the decay amplitudes.[7] Later, we shall have to make such assumptions, in order to reduce the number of parameters used to fit the distributions.

A neutral K meson propagating in liquid hydrogen behaves as a linear superposition of two states with well-defined masses and lifetimes, which we call K_S and K_L. The K meson state at a proper time t after production is therefore given by

$$|K(t)\rangle = P \exp\left[-(\tfrac{1}{2}\lambda_S + im_S)t\right]|K_S\rangle + Q \exp\left[-(\tfrac{1}{2}\lambda_L + im_L)t\right]|K_L\rangle$$
$$\equiv P\, e_S(t)\,|K_S\rangle + Q e_L(t)|K_L\rangle\,, \qquad (8)$$

where λ_S^{-1} and λ_L^{-1} are the lifetimes of K_S and K_L and m_S and m_L are their masses (in units such that $\hbar = c = 1$)[8]. The constants P and Q are determined by initial conditions.

With sufficient accuracy for this experiment, the states K_S and K_L are simply the eigenstates of CP:

$$|K_S\rangle = 1/\sqrt{2}\,(|K^0\rangle + |\bar{K}^0\rangle), \qquad (9)$$
$$|K_L\rangle = 1/\sqrt{2}\,(|K^0\rangle - |\bar{K}^0\rangle).$$

CP violation and regeneration in liquid hydrogen give negligible corrections to Eq. (9).

If a $\bar{K}^0$ state is produced at t=0, we have

$$|K(0)\rangle = |\bar{K}^0\rangle = 1/\sqrt{2}\,(|K_S\rangle - |K_L\rangle), \qquad (10)$$

so $P = 1/\sqrt{2}$, $Q = -1/\sqrt{2}$, and

$$|K(t)\rangle = (1/\sqrt{2})e_S(t)|K_S\rangle - (1/\sqrt{2})e_L(t)|K_L\rangle$$
$$= \frac{1}{2}\, e_S(t)\,(|K^0\rangle + |\bar{K}^0\rangle) - \frac{1}{2}\, e_L(t)(|K^0\rangle - |\bar{K}^0\rangle). \qquad (11)$$

Let a and $\bar{a}$ be the amplitudes for K^0 and $\bar{K}^0$ decay into a particular leptonic charge, spin, and momentum configuration. Then the amplitude for decay at time t into that configuration is, from Eq. (11),

$$M(t) = \tfrac{1}{2}e_S(t)\ \ (a+\bar{a}) - \tfrac{1}{2}e_L(t)\ \ (a-\bar{a}), \tag{12}$$

and the observed differential rate of this decay is

$$d\Gamma(t) = |M(t)|^2 \epsilon\, d\rho = \tfrac{1}{4}\,|e_S(t)\ (a+\bar{a}) - e_L(t)(a-\bar{a})|^2 \epsilon\, d\rho \tag{13}$$

where $d\rho$ is the phase-space element and ϵ is the detection efficiency as a function of the final-state configuration. Thus

$$d\Gamma(t) = \tfrac{1}{4}\left[\,|e_S(t)|^2|a+\bar{a}|^2 + |e_L(t)|^2|a-\bar{a}|^2 - 2\,\mathrm{Re}\left\{e_S(t)\,e_L^*(t)\ (a+\bar{a})\ (a^*-\bar{a}^*)\right\}\right]\epsilon\, d\rho. \tag{14}$$

The observed rate of decay into a given charge state, summed over final-state spins (σ) and momenta, is therefore

$$\Gamma(t) = \tfrac{1}{4}\left[\exp(-\lambda_S t)\int\sum_\sigma |a+\bar{a}|^2\epsilon\, d\rho + \exp(-\lambda_L t)\int\sum_\sigma |a-\bar{a}|^2\epsilon\, d\rho - 2\,\mathrm{Re}\left\{e_S(t)\,e_L^*(t)\int\sum_\sigma (a+\bar{a})(a^*-\bar{a}^*)\epsilon\, d\rho\right\}\right]. \tag{15}$$

Now
$$e_S(t)\,e_L^*(t) = \exp\left\{-\tfrac{1}{2}(\lambda_S+\lambda_L)t\right\}(\cos\delta t - i\sin\delta t), \tag{16}$$

where $\delta = m_S - m_L$, so the time-dependent rate takes the form

$$\Gamma(t) = A\exp(-\lambda_S t) + B\exp(-\lambda_L t) + (C\cos\delta t + D\sin\delta t)\exp\left\{-\tfrac{1}{2}(\lambda_S+\lambda_L)t\right\},$$

where

$$A = \tfrac{1}{4}\int\sum_\sigma |a+\bar{a}|^2\epsilon\, d\rho,\quad B = \tfrac{1}{4}\int\sum_\sigma |a-\bar{a}|^2\epsilon\, d\rho, \tag{17}$$
$$C = -\tfrac{1}{2}\int\sum_\sigma (|a|^2 - |\bar{a}|^2)\epsilon\, d\rho,\quad D = -\int\sum_\sigma \mathrm{Im}(a^*\bar{a})\epsilon\, d\rho.$$

To distinguish the four leptonic decay modes, we add subscripts in Eq. (17), representing the appropriate lepton:

$$\Gamma_{e^+}(t) = A_{e^+}\exp(-\lambda_S t) + B_{e^+}\exp(-\lambda_L t) + (C_{e^+}\cos\delta t + D_{e^+}\sin\delta t)\exp\left\{-\tfrac{1}{2}(\lambda_S+\lambda_L)t\right\}, \tag{18}$$

where $A_{e^+} = \tfrac{1}{4}\int\sum_\sigma |a_{e^+} + \bar{a}_{e^+}|^2\epsilon_{e^+}\, d\rho_{e^+}$, etc., and similarly for Γ_{e^-}, Γ_{μ^+}, and Γ_{μ^-}.

B. CPT Invariance.

In the absence of assumptions about the decay amplitudes, the 16 real parameters A_{e+}, A_{e-}, $A_{\mu+}$, $A_{\mu-}$, B_{e+},....., $D_{\mu-}$ are required to describe completely the time-dependent leptonic decay rates. However, we shall assume that the decay processes are CPT-invariant. Then we see as follows that only eight of these parameters are independent.

Consider, for example, the amplitude a_{e-}, for $K^o \to \pi^+ e^- \bar{\nu}$. Under CP transformation, the process $K^o \to \pi^+ e^- \bar{\nu}$ becomes $\bar{K}^o \to \pi^- e^+ \nu$, for which the amplitude is $\bar{a}_{e+}$. Thus

$$a_{e-} \xrightarrow{CP} \bar{a}_{e+} \tag{19}$$

Now under time-reversal, T, the process $\bar{K}^o \to \pi^- e^+ \nu$ becomes $\pi^- e^+ \nu \to \bar{K}^o$. Since there are no strong final-state interactions, the Watson theorem[9] tells us that, to order α, the amplitude for $\pi^- e^+ \nu \to \bar{K}^o$ is $\bar{a}^*_{e+}$. Thus, with sufficient accuracy,

$$\bar{a}_{e+} \xrightarrow{T} \bar{a}^*_{e+}, \tag{20}$$

and, altogether,

$$a_{e-} \xrightarrow{CPT} \bar{a}^*_{e+}. \tag{21}$$

Hence CPT invariance implies

$$a_{e-} = \bar{a}^*_{e+}, \tag{22}$$

and similary

$$\bar{a}_{e-} = a^*_{e+},\ a_{\mu-} = \bar{a}^*_{\mu+},\ \text{and}\ \bar{a}_{\mu-} = a^*_{\mu+}. \tag{23}$$

Now, in Eq. (18), the phase-space is independent of the charge configuration, so

$$d\rho_{e+} = d\rho_{e-} = d\rho_e \ \text{and}\ d\rho_{\mu+} = d\rho_{\mu-} = d\rho_\mu. \tag{24}$$

Furthermore, in our experiment, the detection efficiency is

independent of the lepton charge, so

$$\epsilon_e^+ = \epsilon_e^- = \epsilon_e \text{ and } \epsilon_\mu^+ = \epsilon_\mu^- = \epsilon_\mu . \tag{25}$$

Combining Eq. (17) with Eqs. (22) to (25), we see

$$\begin{aligned} A_e^- &= A_e^+ \quad , \quad B_e^- = B_e^+, \\ C_e^- &= -C_e^+ \quad , \quad D_e^- = D_e^+, \\ A_\mu^- &= A_\mu^+ \quad , \quad B_\mu^- = B_\mu^+, \\ C_\mu^- &= -C_\mu^+ \quad , \quad D_\mu^- = D_\mu^+. \end{aligned} \tag{26}$$

C. Current-current Interaction.

We shall consider the leptonic neutral K decays within the conventional framework of weak interaction theory, i.e. as current-current interactions with a universal lepton current

$$L_\lambda = \sum_{\ell=e,\mu} \bar{\psi}_\ell \, \gamma_\lambda (1+\gamma_5) \psi_\nu \quad . \tag{27}$$

Then if J_λ is the hadron current, the relevant amplitudes are

$$\left.\begin{aligned} a_\ell^+ &= \langle \pi^- | J_\lambda | K^0 \rangle \langle \ell^+ \nu | L_\lambda | 0 \rangle = \bar{a}_\ell^{-*} \\ \text{and} \\ \bar{a}_\ell^+ &= \langle \pi^- | J_\lambda | \bar{K}^0 \rangle \langle \ell^+ \nu | L_\lambda | 0 \rangle = a_\ell^{-*} \end{aligned}\right\} \ell = \text{e or } \mu \tag{28}$$

Since the only four-vectors associated with the hadrons are their momenta, K_λ and π_λ, the most general matrix elements of J_λ are $\langle \pi^- | J_\lambda | K^0 \rangle = f_+(q^2)(K_\lambda + \pi_\lambda) + f_-(q^2)(K_\lambda - \pi_\lambda) \equiv f_+ p_\lambda + f_- q_\lambda$ (29)

and $\langle \pi^- | J_\lambda | \bar{K}^0 \rangle = g_+ p_\lambda + g_- q_\lambda$,

where $q^2 = 2(m_K^2 + m_\pi^2) - p^2$ is the only scalar variable, and the form factors f_+, f_-, g_+, and g_- are in general complex functions of q^2.

Next we introduce the form-factor ratios

$$x(q^2) = g_+/f_+ , \quad y(q^2) = g_-/f_+ , \quad \xi(q^2) = f_-/f_+ , \tag{30}$$

so that

$$\langle \pi^- | J_\lambda | K^o \rangle = f_+(q^2)\ (p_\lambda + \xi q_\lambda)$$

and

$$\langle \pi^- | J_\lambda | \bar{K}^o \rangle = f_+(q^2)\ (xp_\lambda + yq_\lambda). \qquad (31)$$

Experiments on K_L leptonic decays[10] have revealed no significant q^2-dependence of the quantity of $(\xi+y)/(1+x)$, which suggests that x, y, and ξ are approximately constant in the region of physical q^2. Theoretical considerations[11] support this suggestion, so we take x,y, and ξ to be constants.

Furthermore, we neglect the possibility of fortuitous cancellations and take the observation that $|(\xi+y)/(1+x)| \lesssim 1$ to indicate that $|\xi|\ ,\ |y| \lesssim 1$. Then the terms involving q_λ are not dominant, and indeed we show as follows that they make only a small contribution.

We have $q_\lambda \langle \ell^+ \nu | L_\lambda | 0 \rangle = q_\lambda\, \bar{u}_\ell\, \gamma_\lambda (1+\gamma_5)\, u_\nu$

$$= \bar{u}_\ell\ \gamma_\lambda\ q_\lambda\ (1+\gamma_5)\ u_\nu\ , \qquad (32)$$

where u_ℓ and u_ν are free Dirac spinors. But

$$q_\lambda = K_\lambda - \pi_\lambda = \ell_\lambda + \nu_\lambda \qquad (33)$$

where ℓ_λ and ν_λ are the lepton and neutrino four-momenta, so, applying the Dirac equations,

$$\bar{u}_\ell\ \gamma_\lambda\ \ell_\lambda = m_\ell\ \bar{u}_\ell \text{ and } \gamma_\lambda\ \nu_\lambda u_\nu = 0, \qquad (34)$$

we see that

$$q_\lambda \langle \ell^+ \nu | L_\lambda | 0 \rangle = m_\ell \bar{u}_\ell\ (1+\gamma_5) u_\nu\ . \qquad (35)$$

Thus the terms involving q_λ represent induced scalar (and pseudoscalar) couplings, which are suppressed by the factor m_ℓ. In the vector couplings, i.e. the terms involving p_λ, on the other hand, the corresponding factor is $\sim m_K$. We therefore neglect the sca-

lar couplings in the electronic decays ($m_e/m_K \simeq 0.1\ ^{o}/_{o}$), and consider them only to first order in the muonic modes ($m_\mu/m_K \simeq 20\ ^{o}/_{o}$).

Very great simplifications may now be made in the parameterization of the decay time distributions. In the electronic decays, we write

$$p_\lambda \langle e^+ \nu_e | L_\lambda | 0 \rangle = V_e \tag{36}$$

so that $a_{e^+} = f_+(q^2)\, V_e, \qquad \bar{a}_{e^+} = x\, f_+(q^2)\, V_e = x\, a_{e^+},$ (37)

and Eq. (17) gives

$$A_{e^+} = A_{e^-} = I_e\, |1 + x|^2, \quad B_{e^+} = B_{e^-} = I_e |1 - x|^2, \tag{38}$$

$$C_{e^+} = -C_{e^-} = -2I_e\, (1 - |x|^2), \quad D_{e^+} = D_{e^-} = -4\, I_e \mathrm{Im}(x),$$

where

$$I_e = \tfrac{1}{4} \int \sum_\sigma |f_+|^2 V_e^{\,2}\, \epsilon_e\, d\rho_e. \tag{39}$$

In the muonic decays, we write

$$p_\lambda \langle \mu^+ \nu_\mu | L_\lambda | 0 \rangle = V_\mu \text{ and } q_\lambda \langle \mu^+ \nu_\mu | L_\lambda | 0 \rangle = S_\mu \tag{40}$$

so $$a_{\mu^+} = f_+(q^2)\, (V_\mu + \xi S_\mu) \tag{41}$$

and $$\bar{a}_{\mu^+} = f_+(q^2)\, (x V_\mu + y\, S_\mu).$$

Then, for example,

$$|a_{\mu^+} + \bar{a}_{\mu^+}|^2 = |f_+|^2 \left[V_\mu^{\,2} |1 + x|^2 + 2 V_\mu S_\mu \mathrm{Re}\{(1 + x^*)(\xi + y)\} \right] \tag{42}$$

to first order in S_μ, so that

$$A_{\mu^+} = I_\mu \left[|1 + x|^2 + 2\, K\, \mathrm{Re}\{(1 + x^*)\, (\xi + y)\} \right], \tag{43}$$

where

$$I_\mu = \tfrac{1}{4} \int \sum_\sigma |f_+|^2 V_\mu^2\, \epsilon_\mu\, d\rho_\mu$$

and $$K = \tfrac{1}{4} \int \sum_\sigma |f_+|^2 V_\mu S_\mu \epsilon_\mu\, d\rho_\mu / I_\mu.$$

For reasonable forms of ϵ_μ, $K \sim S_\mu/V_\mu \sim 0.2$, so we write Eq. (43) as

$$A_{\mu^+} = I_\mu\, |(1 + K\xi) + (x + K y)|^2 \tag{44}$$

to first order in K. Similarly,

$$B_{\mu}+ = I_{\mu}\left[|1-x|^2 + 2K\,\mathrm{Re}\{(1-x^*)(\xi-y)\}\right]$$
$$= I_{\mu}|(1+K\xi) - (x+Ky)|^2,$$
$$C_{\mu}+ = -2I_{\mu}\left[1 + 2K\,\mathrm{Re}(\xi) - |x|^2 - 2K\,\mathrm{Re}(x^*y)\right] \qquad (45)$$
$$= -2I_{\mu}(|1+K\xi|^2 - |x+Ky|^2),$$
and $$D_{\mu}+ = -4I_{\mu}\,\mathrm{Im}(x + Ky + K\xi^*x)$$
$$= -4I_{\mu}\,\mathrm{Im}\left[(1+K\xi)^*(x+Ky)\right].$$

We conclude that, to first order in the scalar couplings, we may write

$$A_{\mu}+ = A_{\mu}- = I'_{\mu}|1+x'|^2,\ B_{\mu}+ = B_{\mu}- = I'_{\mu}|1-x'|^2, \qquad (46)$$
$$C_{\mu}+ = -C_{\mu}- = -2I'_{\mu}(1-|x'|^2),\ D_{\mu}+ = D_{\mu}- = -4I'_{\mu}\mathrm{Im}(x'),$$

where

$$I'_{\mu} = I_{\mu}|1+K\xi|^2$$
$$= \tfrac{1}{4}\int_{\sigma}|f_+|^2 V_{\mu}\left[V_{\mu} + 2S_{\mu}\mathrm{Re}(\xi)\right]\epsilon_{\mu}\,d\rho_{\mu}, \qquad (47)$$

and

$$x' = (x + Ky)/(1 + K\xi), \qquad (48)$$

so
$$x' = x + K(y - \xi x). \qquad (49)$$

Thus the parameterizations for the electronic and muonic decays are formally the same, but we cannot a priori take x and x' to be equal.

D. The $\Delta S = \Delta Q$ Rule.

Our main object in this experiment was to test the selection rule $\Delta S = \Delta Q$ for the strangeness-changing hadron current J_{λ}. The status of this rule was discussed in the Introduction. When applied to the neutral K leptonic decays, it requires the following matrix elements to vanish: $\langle\pi^-|J_{\lambda}|\overline{K}^0\rangle$ ($\Delta S = -\Delta Q = +1$) and $\langle\pi^+|J_{\lambda}|K^0\rangle$ ($\Delta S = -\Delta Q = -1$). Since we have assumed CPT invariance, these two are simply related by complex conjugation, and in Eq. (30) we must set

$$g_+ = g_- = 0, \tag{50}$$

so
$$x = y = 0 \tag{51}$$

and
$$x = x' = 0. \tag{52}$$

Then $A_{\ell\pm} = B_{\ell\pm} = \mp\frac{1}{2} C_{\ell\pm}$, $D_{\ell\pm} = 0$, (53)

and the decay time distributions take the simple form (54)

$$\Gamma_{\ell\pm}(t) = I\left[\exp(-\lambda_S t) + \exp(-\lambda_L t) \mp 2\cos\delta t \exp\left\{-\tfrac{1}{2}(\lambda_S+\lambda_L)t\right\}\right]$$

where $I=I_e$ for electronic and $I=I'_\mu$ for muonic decays.

E. CP Invariance.

As we mentioned in the Introduction, a theory proposed by Sachs, discussed in detail in Appendix A, supposes that the CP-violating decays $K_L \Rightarrow \pi^+\pi^-$ and $K_L \rightarrow \pi^o\pi^o$ take place owing to a gross violation of CP in the leptonic neutral K decays. An important part of our experiment is therefore a test of CP conservation in these decay modes.

Since we have assumed CPT invariance, the operators CP and T are equivalent. We saw in Section IIB that, to order α, the decay amplitudes are complex-conjugated under time reversal. In the current-current formulation of the decay interaction, this means that $f_+ = f_+^*$, $f_- = f_-^*$,

$$g_+ = g_+^* \text{ and } g_- = g_-^* \tag{55}$$

in Eq. (30). Thus

$$x = x^*,\ y=y^*,\ \xi=\xi^*, \tag{56}$$

and

CP invariance implies that x and x' are real. (57)

Since the $\Delta S = \Delta Q$ rule implies that x and x' vanish, CP violation can only be observed in the leptonic decay time distri-

butions if this rule is also violated. However, if the $\Delta S = \Delta Q$ rule is valid, the Sachs mechanism cannot operate, so this limitation does not affect our test of the Sachs model of $K_L \not\to 2\pi$.

F. Summary.

We have seen that the time distributions of the neutral K leptonic decays have the general form

$$\Gamma_\ell^{\pm}(t) = A_\ell^{\pm} \exp(-\lambda_S t) + B_\ell^{\pm} \exp(-\lambda_L t) + (C_\ell^{\pm} \cos\delta t + D_\ell^{\pm} \sin \delta t) \exp\left\{-\tfrac{1}{2}(\lambda_S+\lambda_L)t\right\}, (\ell = e \text{ or } \mu) \qquad (17)$$

involving sixteen real parameters A_e^+, A_e^-, ..., D_μ^-.

By assuming a CPT-invariant, universal current-current decay interaction with constant form factor ratios, we have expressed these in terms of two real parameters, I_e and I'_μ, and two complex, x and x', as shown in Eqs. (38) and (46). The electronic parameter x is the ratio of the vector interaction form factors for the $\Delta S/\Delta Q = -1$ and $+1$ amplitudes. The corresponding muonic parameter, x', is expressed in terms of the form factor ratios as

$$x' = x + K\,(y - \xi x) \qquad (49)$$

where $K \sim 0.2$; the second term represents the first-order contribution of the induced scalar interaction.

Finally, we have seen that the $\Delta S = \Delta Q$ rule predicts x and x' to be zero, while CP invariance predicts only that they should be real.

III. EXPERIMENTAL PROCEDURES

A. The Beam

The K^- beam for our experiment was designed and built by Dr. Joseph J. Murray and Mr. Roger O. Bangerter, and it was operated in conjunction with the 25-inch hydrogen bubble chamber at the Bevatron at various times during the period August 1965 to July 1967. Since the beam has been fully described elsewhere,[12] we give here only a brief summary of the relevant features.

Although the K^- momentum of about 400 MeV/c was chosen for reasons irrelevant to the study of neutral K meson decays (namely, for the copious production of polarized Σ hyperons), such a low beam momentum is almost essential to our experiment, since it leads to the production of $\overline{K}^0$ mesons of well-determined, low momenta. In the leptonic decays of these mesons, the decay time is well-determined, the resolution of two- and three-body decay hypotheses is good, and many of the leptons, including some muons, have momenta which are low enough to permit their identification by ionization.

Two major difficulties have to be overcome in the design of a low-momentum K^- beam: the high background to K^- ratio at the target (about 1 000:1) and the decay loss of K^- in the beam (about 10 $^0/_0$ per foot at 400 MeV/c). The shortest possible beam length is about 40 feet, which would lead to a background to K^- ratio of about 50 000:1 at the bubble chamber in an unseparated beam. Two-stage conventional separation might reduce this ratio to 10:1, which would still be unsatisfactory. By using a new electrostatic septum filter, developed for this experiment, we obtained a background to K^- ratio at the bubble chamber of about 1:5.

The filter operates by passing the beam between stacks of closely-spaced high-voltage electrodes, which deflect background particles into uranium bars located between the stacks. It has a K^- transmission of 25 %, and achieves a rejection of the order of 10^5 in less than 7 feet.

Typically, our bubble chamber pictures contained about 6 K^- and 2 background tracks. The background consisted of pions, muons, and some electrons. Since the background tracks had practically minimum ionization, they were easy to distinguish from the K^- tracks, which had 2.6 times minimum ionization.

By movement of our target, and by the use of a beryllium beam degrader, we were able to obtain data in the K^- momentum range 310-430 MeV/c. However, 75 % of the data were taken in the range 370-410 MeV/c.

B. Scanning and Selection of Candidates.

The appearance of a leptonic neutral K decay in our photographs is shown by the solid lines in Fig. 3: the event is characterized by a 0-prong and a V.

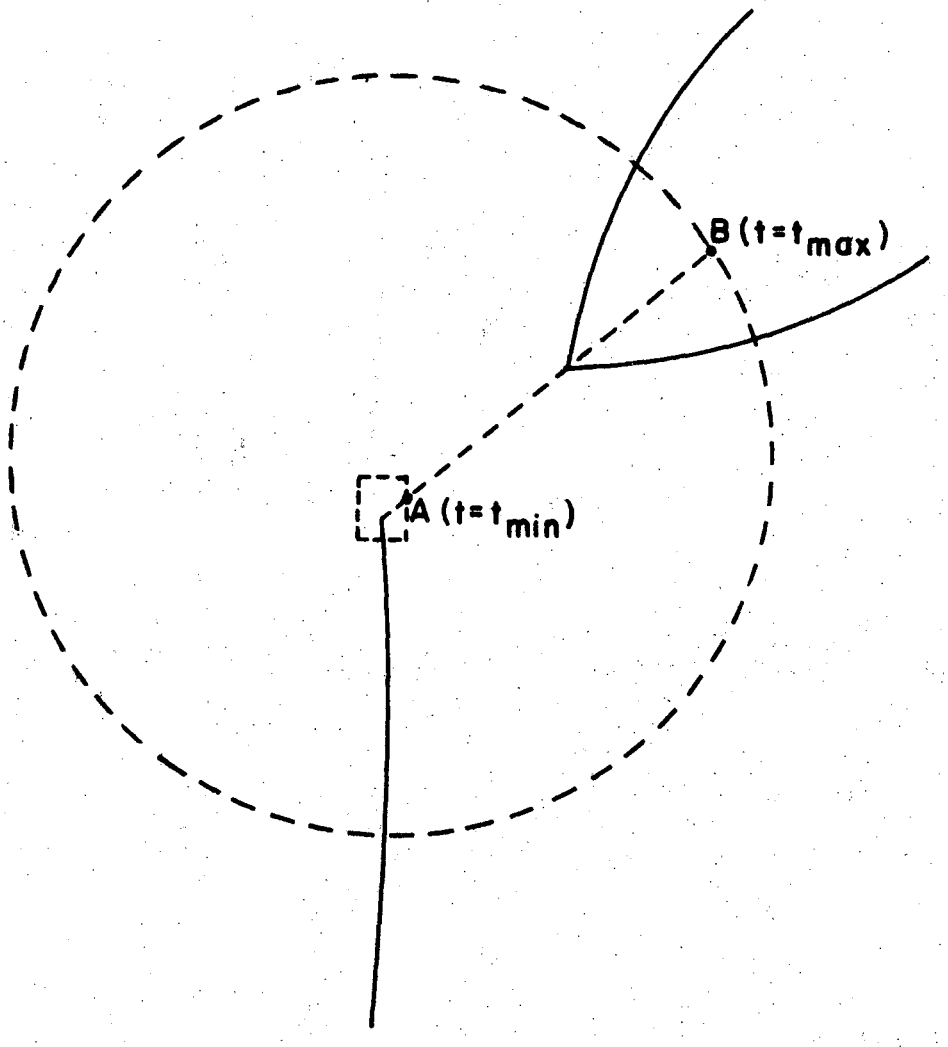

Fig. 3. A typical event, and the times t_{min} and t_{max} for this event.

The pictures were therefore scanned for V's. If both a V and a 0-prong were found, the event was measured on a Spiral Reader or Franckenstein automatic measuring machine, and we used the kinematics fitting program SIOUX to attempt four-constraint (4C) fits to $\overline{K}^{o}$ and Λ production and two-body decay. If the confidence level for the $\overline{K}^{o}$ fit was less than 5×10^{-4} and the V was not identified as a Λ decay during scanning, fits to all three-body K decay hypotheses were tried. If the confidence level for any of these was greater than 0.02, the event was called a three-body K^{o} decay candidate and was remeasured on a Franckenstein measuring machine.

Pictures in which the scanner recorded a V but no 0-prong, and did not definitely identify the V as a Λ decay by ionization or stopping of the positive track, were carefully rescanned for 0-prongs and measured if one was found.

In about 9 $^{o}/_{o}$ of our pictures, there was a V and two or more 0-prongs, none of which was clearly associated with another event. After measuring a sample of these, we found that in 43 $^{o}/_{o}$ of them we could obtain more than one $\overline{K}^{o}$ production and three-body decay fit, in which the same V was associated with different 0-prongs. Since the resolution of such ambiguities is likely to depend on the distance of the V from the various 0-prongs, this could give rise to a bias in the decay time distributions. We avoided this possibility by rejecting from our set of candidates all those in pictures containing extra 0-prongs not clearly associated with other events. In this way we obtained those K^{o}'s which were associated with a unique production vertex, but fit only the 1C $\overline{K}^{o}$ production and three-body decay hypotheses.

C. Geometrical Cuts.

For neutral K decays at very short times after production, the vertex of the V is close to the 0-prong, and the event may be missed because it appears to the scanner to be a 2-prong. At long times, the neutral K approaches the edge of the visible region of the bubble chamber, and the V may not be seen. The time distributions of observed decays are therefore expected to fall off at both very short and long times, owing to our reduced efficiency for detecting decays at these times.

In order to avoid the uncertainties associated with an estimation of this time-dependent detection efficiency, we have used only those decays occurring in a time interval in which we are confident that the detection efficiency is independent of time. This interval is, in general, different for each event, since it depends on the production angles and momenta. Consider, for example, the event in Fig. 3. For a $\overline{K}^0$ produced at this angle, the probability that an event will be misidentified as a 2-prong falls to zero for decay beyond a point A, corresponding to a time of flight t_{min}. Similarly, for a neutral K travelling in this direction, there is no chance that the event will be lost owing to the finite size of the chamber until a point B is reached, at time t_{max}. Thus the detection efficiency is time-independent in the interval from t_{min} to t_{max}. Happily, the decay did in fact occur in this interval, so this event would be retained as a candidate. If the decay occurred before point A or after point B, the event would be rejected. We shall discuss later how the values of t_{min} and t_{max} for the events retained are used in fitting the time distributions.

We calculated t_{min} for each event as follows: the point A is that point on the neutral K track whose projection onto the x-y plane lies on a rectangle enclosing the 0-prong, as shown in Fig. 3. In the 25-inch bubble chamber coordinate system, the z-axis points towards the cameras, so the x-y projection represents a rough average of the three camera views. We found the correct dimensions for the rectangle by noting that the two-body neutral K decays, $K_S \rightarrow \pi^+\pi^-$, are subject to the same loss of scanning efficiency at short decay times. We therefore took a sample of 5000 two-body decays and assigned a value of t_{min} to each one according to the above prescription, for various sizes of the rectangle. Those with a decay time less than t_{min} were rejected, and those remaining were given a weight $\exp(\lambda_S t_{min})$. As the dimensions of the rectangle were increased, the sum of the weights of the remaining events increased, indicating the loss of short-time decays, and then became constant for values at which the events outside the rectangle had the correct exponential decay time distribution. In this way, we found that a rectangle extending 3.5mm ahead of the 0-prong, 2.5mm behind it, and 1.75mm to each side gave values of t_{min} at which the detection efficiency was indeed independent of time, and these were the dimensions we used to calculate t_{min} for the leptonic decays.

If the decay vertex is close to the edge of the visible region of the bubble chamber, there are three distinct ways in which the probability of detection may be reduced. First, the scanner may not notice the V. This loss mechanism should be significant only at distances of less than about 3 cm from the edge of the visible region. Second, the lepton track in a leptonic decay may be so short that it is difficult to determine its ionization. This mechanism may be

regarded as decreasing the detection efficiency for events in which the lepton is identified by ionization, and correspondingly increasing the efficiency for events in which the lepton is unidentified. This effect is discussed further in Section III E; it suffices to state here that we do not believe this to be the dominant loss mechanism at large decay times. The third mechanism, which we regard as dominant in the sense that it determines the value of t_{max} for each event, involves a loss of momentum resolution for short decay tracks.[13] As will be discussed in the next section, we use several kinematic cuts to eliminate $K_S \to \pi^+\pi^-$ decays from our sample of leptonic decay candidates. The probability that a truly leptonic decay will be rejected by these cuts depends on the various track momenta and angles in the event, and on the associated errors in these quantities. Some of these errors may depend indirectly on the decay time of the neutral K, so the cuts may lead to biases in the decay time distributions of the events that are not rejected.

The dominant errors in our experiment are momentum errors due to multiple Coulomb scattering.[28] Setting errors on tracks and vertices during measurement are typically 5 microns on the film, whereas expected Coulomb point scatters are in the range 5 to 30 microns. Even for the shortest neutral K's, with decay time $t \sim t_{min}$, the production angle is so well determined that the $\overline{K}^o$ momentum error is dominated by the uncertainty in the K^- momentum. This uncertainty is not correlated with the decay time of the neutral K, so we do not expect the neutral K momentum error to be a source of time-dependent bias. The momentum error for a decay track, on the other hand, depends on the length, on the film, of the measured track segment in the three camera views. Of necessity, this

length is smaller for decay vertices near the edge of the visible region, so the momentum error is correspondingly larger. For decay vertices well inside the visible region, the decay track momentum errors are small, and the neutral K momentum error dominates: this is not expected to produce a time-dependent bias. As we approach the limits of the visible region, however, the decay track momentum errors become dominant, and there is a possibility of bias.

We may even make a crude estimate of the cross-over point, where the neutral K and decay track errors are comparable. When the errors are mainly due to multiple Coulomb scattering, the momentum error for a track of length ℓ^{cm} and dip angle λ is approximately given by[14]

$$\frac{\delta p}{p} \approx \frac{1}{B\beta\sqrt{\ell}\,\cos\lambda}\,, \tag{58}$$

where $c\beta$ is the velocity of the particle and B is the magnetic field in kilogauss. Other quantities, such as the radiation length, have been absorbed in the numerical factor of order unity. Thus

$$\delta p \approx \frac{E}{cB\sqrt{\ell}\,\cos\lambda}\,, \tag{59}$$

where E is the total energy of the particle. According to the argument given above, the error in the neutral K momentum is

$$\delta p_{K^o} \sim \frac{E_{K^-}}{cB\sqrt{\ell_{K^-}}}\,, \tag{60}$$

the error in the K^- momentum, while the momentum error for a decay track is

$$\delta p_d \approx \frac{Ed}{cB\sqrt{\ell_d}\,\langle\cos\lambda_d\rangle} \approx \frac{\sqrt{2}\,Ed}{cB\sqrt{\ell_d}}\,. \tag{61}$$

At the cross-over point, we have $\delta p_{K^o} \sim \delta p_d$, which gives

$$\ell_d \sim 2 \left(\frac{E_d}{E_{K^-}}\right)^2 \ell_{K^-} \qquad (62)$$

Taking $E_{K^-} = 640$ MeV, and typical values of $E_d \sim 200$ Mev and $\ell_{K^-} \sim 25$ cm, we obtain

$$\ell_d \sim 5 \text{ cm.} \qquad (63)$$

We may conclude from this very approximate calculation that there is a possibility of bias for decays at distances less than or of the order of 5 cm from the edge of the visible region.

The argument given above is not sufficiently precise to form a reliable basis for a cut. To make a more precise calculation of the region in which this loss mechanism is significant, we have used a Monte Carlo simulation of our experiment. Fortunately, we find that this region does in fact extend only 5 cm from the edge of the visible region of the chamber.

For all the computer simulation in our experiment, we have used the new Lawrence Radiation Laboratory program PHONY.[15] This program reduces Monte Carlo events to sets of coordinate points, simulating the output from a measuring machine. The correct Coulomb scattering and measurement error distributions are used to compute for each point a displacement from an unscattered particle trajectory. This feature allowed us to study precisely the loss of leptonic decays through the mechanism discussed above.

We generated 3616 simulated leptonic decays, with K^- and $\overline{K}^0$ distributions deduced from the real $K_S \to \pi^+\pi^-$ events at the beam momentum setting where we took most of our data. For the decay distributions,

we used the standard current-current interaction matrix element described in Section II C. We assumed $\Delta S = \Delta Q$, setting x=y=0 (see Section II D), and also set $\xi = 0$ in generating the distribution of muonic decays. However, we generated muonic and electronic decays in the ratio of the published $K_L \rightarrow \pi\mu\nu$ and $\pi e\nu$ branching ratios.

We studied the fraction of simulated leptonic decays rejected by our kinematic cuts as a function of the smaller of the projected lengths of the two decay tracks, the plane of projection being the x-y plane defined on p. 21. As expected, the rejected fraction approaches 100 $^{o}/_{o}$ for small projected lengths, but at about 5 cm it becomes stable at 23 $^{o}/_{o}$ and shows no significant variation in the range 5-20 cm.

By means of a cut on the dip angles of the decay tracks and an appropriate choice of the decay fiducial volume, we have ensured that the projected length of a decay track is never limited to less than 6 cm by the boundaries of the visible region of the chamber. We reject events in which either decay track has a dip angle greater than 55 deg or less than -55 deg. The boundaries of the fiducial volume are at least 6 cm from the limits of the visible region, and those boundaries that are parallel to the x-y plane, that is, parallel to the glass windows at the top and bottom of the chamber, are 8.5 cm from the chamber windows, corresponding to a projected distance of 8.5 cot (55 deg) = 6 cm. The point B in Fig. 3, where the neutral K time of flight would be t_{max}, is the point at which the extended neutral K line of flight leaves this fiducial volume. With t_{max} defined in this way, a decay during the time interval from t_{min} to t_{max} always has a projected length of more than 6 cm available for both of the decay tracks, and the

probability of loss is therefore independent of time. Of course, a decay track that stops, decays or interacts inside the chamber may have an actual projected length of less than 6 cm, but, for our choice of t_{max}, the probability of this is independent of time and does not give rise to a bias.

In addition to the minimum length, dip angle and fiducial volume cuts discussed above, we made one further geometrical cut, which should be mentioned before we go on to the kinematic cuts. We rejected events in which the opening angle of the V was less than 2 deg or greater than 170 deg. At the smaller angles, this cut removed a large number of conversion electron pairs. At large angles, it eliminated most of the "events" in which the V was in fact the decay or small-angle scattering of an incoming charged particle, and the 0-prong just happened to occur in the same picture and to be unassociated with a genuine decay V. We also have kinematic cuts to remove events which, after visual examination, could be this type of background, but the simple opening angle criterion greatly reduced the number of spurious events we had to look at.

D. Elimination of Background.

In Table II we have listed the processes, other than leptonic neutral K decay, which may have the appearance of a 0-prong and a V, and which therefore constitute possible sources of background in our experiment. Also listed are estimates, sometimes very approximate, of the number of events of each type occurring inside our decay fiducial volume. We show all processes for which one or more events are expected.

Very large numbers of potential background events were eliminated by the preliminary selection criteria and geometrical cuts discussed in

Sections II B and C, for reasons that should be clear from that discussion. Nevertheless, at this stage of the analysis we had 758 leptonic decay candidates, of which less than one half were expected to be true leptonic decays. Most of the other events were $K_S \to \pi^+\pi^-$ decays which for some reason failed the 4C $\overline{K}^o$ production and two-body decay fit. A number of circumstances may lead to the failure of this fit. First, a decay pion may decay or Coulomb scatter in flight, and the measurer may not observe the kink in the track at the point where this occurred, and may measure the track beyond this point. This gives an incorrect determination of the track angles and momentum, which may cause the event to fail. Second, one or more photons of significant momentum may be emitted during the decay. We estimate that a photon momentum in the decay centre-of-mass frame, k, of more than 4 MeV/c may spoil the two-body decay fit. Third, even if the decay is not radiative and the decay tracks have no kinks, the $\overline{K}^o$ production process may be radiative or the K^- may scatter before interacting. In the table, we refer to both of these situations as abnormal $\overline{K}^o$ production. Finally, the neutral K may scatter in flight.

We removed nearly all of this background due to $K_S \to \pi^+\pi^-$ by means of the following three cuts. We discuss later, on p. 32, the effects of our cuts on leptonic decays.

(a) We made 1C fits to $\overline{K}^o$ production and two-pion decay, in which first one and then the other pion was considered unmeasured. Clearly, an otherwise good two-body decay with one bad pion track should give a good fit when the bad track is not used. Furthermore, in such a fit the initial momentum and direction of the "unmeasured" pion are reconstructed by momentum conservation from the other tracks, and, if the

Table II. Possible Sources of Background

N_b is the approximate number of events expected inside our fiducial volume. N_a is the number expected to remain after our selection procedures for leptonic decays.

Type of event	N_b	N_a
(1) $K^- p \to \overline{K}^o n$; $K_S \to \pi^+\pi^-$	20 000	0
(1) with: π Coulomb scattering $\gtrsim 1$ deg.	500	0.5
π decaying at $\lesssim 5$ deg.	90	0
both π Coulomb scattering	6	0
one π scattering, one π decaying	1	0
K^o scattering	80	0
(2) Abnormal $\overline{K}^o$ production; $K_S \to \pi^+\pi^-$	300	0
(2) with: π Coulomb scattering	8	0
π decaying	1	0
(3) $K^- p \to \overline{K}^o n$; $K_S \to \pi^+\pi^-\gamma$ ($k > 4$ MeV/c)	400	31.4
(3) with: π Coulomb scattering	10	0
π decaying	2	0
(4) Abnormal $\overline{K}^o$ production; $K_S \to \pi^+\pi^-\gamma$	6	1
(5) $K^- p \to \overline{K}^o n$; $K_S \to \pi^+\pi^-\gamma\gamma$ (both $k > 4$MeV/c)	3	0.5
(6) $K^- p \to \overline{K}^o n$; $K_L \to \pi^+\pi^-\pi^o$	50	0
(7) $K^- p \to$ 0-prong; $\gamma \to e^+e^-$	1 600	0
$\pi^o \to \gamma\, e^+e^-$	700	0
$\Lambda \to p\pi^-$	75 000	0
wall K_L decay	20	0.5
V not a neutral decay	5 000	0
other Λ decay modes	800	0

bad track had a small decay or scattering kink, it should still lie close to this reconstructed direction. We show in Appendix B that the appropriate criterion of "closeness" is the quantity $F = P_{fit}\,\beta_{fit}\,\Delta\theta$, where p_{fit} is the reconstructed momentum, $c\beta_{fit}$ is the corresponding velocity, and $\Delta\theta$ is the space angle between the measured and reconstructed initial directions of the track.[16] It is also shown in Appendix B that all except 0.5 of the Coulomb scatterings, and all of the decays, on the pion tracks should give values of F less than 2200 (MeV/c) deg. We therefore rejected all events giving a fit of this kind with confidence level greater than 1.5×10^{-3} and F less than 2200 (MeV/c) deg.

(b) To remove most of the radiative decays, we made a 1C fit to $\overline{K}^{o}$ production and $\pi^{+}\pi^{-}\gamma$ decay. Unfortunately, muonic decay events have a tendency to fit this hypothesis, because of the similarity of the pion and muon masses, so we could not simply reject all events for which a fit was obtained. However, the great majority of radiative decays produce a photon of very low momentum in the centre-of-mass frame, while the neutrino spectrum in muonic decay is expected to approach zero at low momenta. We therefore compromised by rejecting events for which this fit had a confidence level greater than 1.5×10^{-3} and a centre-of-mass photon momentum less than 50 MeV/c. This left a small number of radiative decays with photons of higher momentum, for which we had to correct our leptonic decay distributions. The calculation of this correction is discussed in Section IV A.

(c) A significant number of two-pion decays failed the normal fit for more than one reason, giving rise to "second-order" background.

The principal sources of these events were (1) $\pi^+\pi^-$ decays in which both decay pions Coulomb scattered, (2) $\bar{K}^0$'s produced radiatively or after K^- scattering (abnormal production) and decaying to $\pi^+\pi^-\gamma$ or to $\pi^+\pi^-$ followed by pion scattering, (3) $\pi^+\pi^-\gamma$ decays followed by pion scattering, and (4) $\pi^+\pi^-\gamma\gamma$ decays. We expect less than 3 events of these types to have decay photons with centre-of-mass momenta greater than 10 MeV/c, or pion scattering with F (see p.29) greater than 376 (MeV/c) deg. We therefore made a special fit in which we increased the errors on the tracks of the V, to take into account the possible emission of 10 MeV/c photons in the decay and a subsequent scattering with F=376 (MeV/c) deg. This 3C fit was to the two-pion decay of a neutral K coming from the direction of the 0-prong; we did not use the momentum or direction of the beam track, so second-order background events with a bad beam track or radiative production vertex should also give a good fit. We rejected all events giving a confidence level greater than 0.1 for this special fit. In view of the large kinematic overlap between this cut and the preceding two, we estimate that less than 1.5 second-order background events should remain after the application of all three cuts.

Details of the calculation of the error increases for the V tracks are given in Appendix C.

Having made the above cuts, we were left with 452 candidates, which we examined on a scanning table. We could then make a number of cuts which depended in part on the results of this examination.

(d) One-constraint fits to the two-body decay of a Λ or neutral K of unknown origin were made. An event was rejected if it gave a

confidence level greater than 5×10^{-4} and the appearance of the V was consistent with the corresponding interpretation. This cut eliminated two-body decays in which the beam track measurement was bad, the production process was radiative, or the neutral particle scattered or interacted in flight. It also eliminated two-body "wall V's," that is, decays of neutral particles produced outside the visible region which were mistakenly associated with a 0-prong in the picture.

(e) The tracks of the V were interpreted as electrons, if this was consistent with their ionization, and the invariant mass of the pair was calculated. If this was less than 140 MeV, the event was rejected. This cut removed gamma-ray conversion pairs, and also decays of the forms $K_S \to \pi^o\pi^o$, $\pi^o \to e^+e^-\gamma$ and $\Lambda \to n\pi^o$, $\pi^o \to e^+e^-\gamma$.

(f) In some events, it could not be definitely established by inspection that both particles in the V were moving out from the vertex. This raised the possibility that the V was the decay of an incoming muon, or the decay or elastic scattering of an incoming charged pion. When a V appeared to be consistent with one of these hypotheses, we calculated the missing mass at the vertex with the appropriate track reversed, and, for the π and μ decays, rejected the event if the square of this lay within four standard deviations of a correct value (0 for the pion decay and the range 0 to $(105\text{MeV})^2$ for the muon decay). For the pion scattering hypothesis, we also required the recoiling proton to be invisible (missing momentum squared within four standard deviations of the range 0 to $(80\ \text{MeV/c})^2$) before rejecting an event.

We believe that cuts (a) to (f) cover all significant sources of background in our experiment.[29] The decay mode neutral $K \to \pi^+\pi^-\pi^o$ is

kinematically quite distinct from the leptonic decays and gives rise to no background. In a sample of 1.6×10^5 pictures, we made a search for a three-body wall V's, which might give spurious leptonic fits with unassociated 0-prongs in the same picture. In this sample, there were 29 wall V's inside our decay fiducial volume. For each wall V, we simulated an unassociated 0-prong by measuring a beam track associated with a real event in the same picture. None of the 0-prong plus wall V combinations survived our selection criteria for leptonic decays. Only one had a satisfactory fit to a leptonic hypothesis, namely $\pi\mu\nu$ decay, and this was inconsistent with the ionization of the positive track of the V, which was clearly an electron. From this study, we concluded that the background due to wall V's was negligible. There might be about one such background event in our sample. For this event, all distances between the 0-prong and V would be equally probably, so we may say that it would have K_L time distribution.

We subjected simulated leptonic decays, generated according to the $\Delta S = \Delta Q$ rule, to cuts similar to those applied to our leptonic candidates, and found that about 50 $^{o}/_{o}$ of them were rejected. Those remaining showed no biases in their decay time distribution, and gave good agreement with $\Delta S = \Delta Q$ when analyzed by the methods we shall discuss in Section IV B.

E. Identification of Leptons.

We have been able to identify the lepton in 119 of the 252 events remaining after the selection procedures described in the previous section. Of the identified leptons, 32 were e^+, 49 e^-, 14 μ^+, and 24 μ^-.

We identified 78 of the 81 electrons and 25 of the 38 muons by

comparison of track densities during scanning-table inspection of the events. A computer program was used to predict the projected relative ionization for each mass hypothesis for each track, at the beginning and end of the measured track segment in each of the three camera views. If these predictions were judged to be consistent with the observed event for only one decay hypothesis, the event was considered to be identified, independent of the kinematic confidence levels of the various three-body decay hypotheses. In most cases, all that was required was a comparison of the two tracks of the V: if the track of lower momentum was nevertheless less dense, the decay was clearly leptonic (with some obvious exceptions for steeply-dipping tracks). Comparison with a nearby minimum-ionizing track then usually sufficed to determine whether the lepton was an electron or a muon. Of great assistance in the identification of leptons was the low momentum of our K^- beam, which caused 50 $^{o}/_{o}$ of the leptons to have momenta less than 140 MeV/c.

If a lepton could not be positively identified by inspection, we considered the event to be completely ambiguous between the leptonic and $\pi\pi\gamma$ decay hypotheses. We made no use of kinematic confidence levels in identifying events, because we found evidence from simulated events that the resolution of kinematically similar hypotheses, such as $\pi^+\mu^-\nu$, $\pi^-\mu^+\nu$, and $\pi^+\pi^-\gamma$, depends on the distance between the 0-prong and the V, and hence on the time of flight of the neutral K. We therefore chose to make no resolutions on the basis of kinematics, rather than to introduce a time-dependent resolution function based entirely on a Monte Carlo simulation.

It should be emphasized that for kinematically dissimilar hypotheses, such as leptonic decay and the various kinds of background rejected, often on a kinematic basis, by our cuts, we found no evidence that the resolution depends significantly on the distance between the 0-prong and V, after application of the geometrical cuts discussed in Section III C.

It is clear that leptonic tracks of small projected length cannot be identified, because their ionization cannot be observed with sufficient precision. We believe, however, that the minimum projected length of 6 cm (4 cm on the scanning table) provided by our fiducial volume and dip angle cuts is sufficient to eliminate any significant bias of this kind, and, indeed, the results of our analysis are not significantly affected if we make these cuts more restrictive.

In 3 electronic and 13 muonic decays, identification was made with the help of information other than track density. Sources of information were δ-ray momenta for electrons,[17] and decays and comparison with curvature templates for muons. The probability of obtaining information of these kinds does depend on the position of the decay vertex in the bubble chamber. However, in view of the small number of events identified in these ways, we do not believe that this effect gives rise to a significant bias in the time distributions. Indeed, if we make no use of information other than track density, and treat these 16 events as unidentified, the results of our analysis are not significantly affected.

As a final check that our lepton identification procedures do not introduce biases, we have performed an analysis in which we treat all 252 of our events as unidentified. The results are consistent with those of the full analysis discussed in Section IV B.

An important feature of our selection criteria and methods of lepton identification is that they are all charge symmetric. The numbers of identified positive and negative leptonic decays therefore provide information, as well as the shapes of the decay time distributions. Furthermore, the predicted time distribution of the ambiguous events is proportional to the sum of the positive and negative leptonic decay time distributions, corrected for the expected $\pi^+\pi^-\gamma$ contamination, which we discuss in Section IVA. In Section IVB, we describe how these facts are used in the maximum-likelihood analysis of our data.

IV. ANALYSIS AND RESULTS.

A. Correction for Remaining Background.

As discussed in Section IIID, the principal background remaining after our cuts consists of radiative two-pion decays with centre-of-mass photon momenta greater than 50 MeV/c. These events cannot be satisfactorily removed from our sample of ambiguous events because they are kinematically very similar to muonic decays, so we have had to apply a correction based on theoretical predictions of the number and distributions of radiative decays. We estimate that other sources of background contribute less than 2 events with the K_S lifetime and about 0.5 with the K_L lifetime. We have not corrected for these events.

To compute the correction for radiative two-pion decay, we assume that this process occurs only though inner bremsstrahlung of the mode $K_S \to \pi^+\pi^-$. This hypothesis is supported by earlier experimental data[18] and by our own, which we discuss at the end of this Section. It follows at once that the time distribution of the $\pi^+\pi^-\gamma$ events will be exponential, with the K_S lifetime. The number of events may be obtained by evaluation of the relevant Feynman graphs, which are shown below.

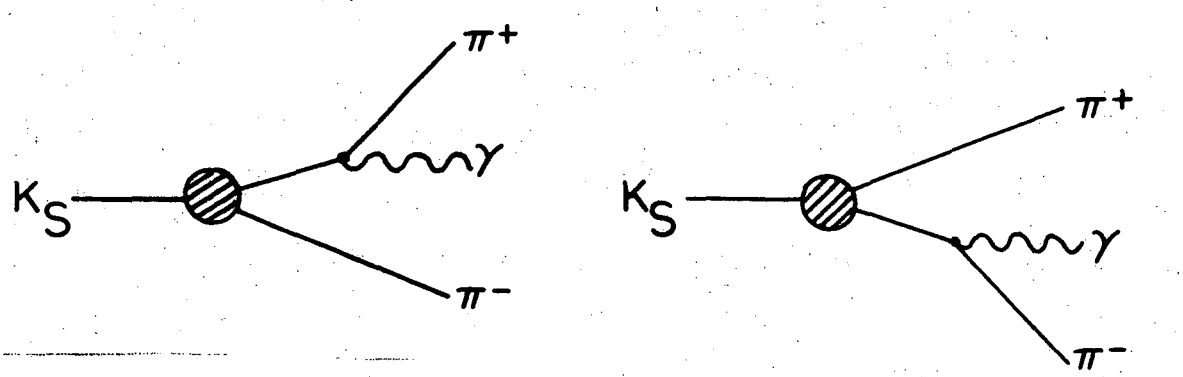

This leads to a differential decay rate given by

$$\frac{d^2\Gamma(K_S \to \pi^+\pi^-\gamma)}{dk\ d(\cos\theta)} = \frac{2\alpha}{\pi}\Gamma(K_S \to \pi^+\pi^-)\ \frac{\beta}{\beta_o}\ \frac{\beta^2\sin^2\theta}{(1+\beta^2\cos^2\theta)^2}\ \frac{1}{k}\left(1-\frac{2k}{m_K}\right), \tag{64}$$

where k is the photon momentum in the overall centre-of-mass system, $c\beta$ is the pion velocity in the dipion centre-of-mass system, and θ is the angle between the photon and the π^+ in the dipion centre-of-mass system. Then k and β are related by the equation

$$1-\frac{2k}{m_K} = 4\frac{m_\pi^2}{m_K^2}\ (1-\beta^2)^{-1} \tag{65}$$

and β_o is the value of β when $k = 0$:

$$\beta_o = \left(1-4\frac{m_\pi^2}{m_K^2}\right)^{+\frac{1}{2}} \tag{66}$$

Integrating Eq. (64) with respect to cos θ, we obtain the centre-of-mass photon spectrum:[19]

$$\frac{d\Gamma(K_S \to \pi^+\pi^-\gamma)}{dk} = \frac{\alpha}{\pi}\Gamma(K_S \to \pi^+\pi^-)\ \frac{\beta}{\beta_o}\left(\frac{1+\beta^2}{\beta}\log\frac{1+\beta}{1-\beta}-2\right)\frac{1}{k}\left(1-\frac{2k}{m_K}\right) \tag{67}$$

Finally, integrating this spectrum over the range of k from 50 MeV/c to the kinematic limit of 170.7 MeV/c, we find

$$\Gamma(K_S \to \pi^+\pi^-\gamma;\ k>50\ \text{MeV/c}) = (2.56\times10^{-3})\,\Gamma(K_S \to \pi^+\pi^-) \tag{68}$$

Since the $\pi^+\pi^-\gamma$ decays should have the same time distribution as the $\pi^+\pi^-$ decays, the predicted number of $\pi^+\pi^-\gamma$ decays is given by

$$n_\gamma = (2.56\times10^{-3})\ \frac{\epsilon_\gamma}{\epsilon_{2\pi}}\ n_{2\pi} \tag{69}$$

Here $\epsilon_{2\pi}$ is the efficiency of any set of cuts which removes all background and scanning biases from our sample of $\pi^+\pi^-$ decays, and $n_{2\pi}$ is the observed number of such decays after these cuts; ϵ_γ is the efficiency of our selection criteria for leptonic decays when applied to

$\pi^+\pi^-\gamma$ decays, that is, the probability that a $\pi^+\pi^-\gamma$ decay will satisfy all of these criteria and be included in our sample of 252 events.

To evaluate $n_{2\pi}$ and $\epsilon_{2\pi}$, we subjected real and simulated $\pi^+\pi^-$ decays to set of cuts designed to eliminate all background and scanning biases. For uniformity, we rejected events having a decay track dip angle greater than 55 deg or less than -55 deg, as we did with the leptonic decays. We found $n_{2\pi}$ = 12 833 after these cuts, and $\epsilon_{2\pi}$ = 66 $^{o}/_{o}$. This low efficiency was due almost entirely to the dip angle cut, which removed 31 $^{o}/_{o}$ of the simulated $\pi^+\pi^-$ decays.

We applied selection criteria similar to those described in Section III to simulated $\pi^+\pi^-\gamma$ decays, and found ϵ_γ = 0.65. This is considerably higher than the estimated efficiency for true leptonic decays, (about 0.50) since the high photon momentum makes $\pi^+\pi^-\gamma$ decays with k >50 MeV/c less likely to be rejected as possible $\pi^+\pi^-$ background.

Since some of our selection criteria involve scanning-table examination of the event, we were unable to estimate ϵ_γ with great precision from simulated events, which could not, of course, be so examined. However, after varying our assumptions about the importance of scanning information within reasonable limits, we are confident that our estimate of ϵ_γ is accurate within 5 $^{o}/_{o}$, which is more than adequate for calculating the required correction to our data.

The predicted number of background $\pi^+\pi^-\gamma$ decays in our sample of 133 ambiguous events is now given by Eq. (69):

$$n_\gamma = 31.4 \text{ events.} \tag{70}$$

In Section IVB we discuss how this number is used to make a correction to the likelihood function in the maximum-likelihood analysis.

We expect a small but significant number of kinematically unambiguous $\pi^+\pi^-\gamma$ decays in our experiment, since we find, from further analysis of simulated events, a probability $\epsilon_{\gamma u} = 0.157$ that a $\pi^+\pi^-\gamma$ decay will satisfy all of our selection criteria, have only three-body decay fits, and have a confidence level for the $\pi^+\pi^-\gamma$ fit that is greater than 2 $^{o}/_{o}$ and more than 50 times greater than that of the second-best fit. This leads to a predicted number $n_{\gamma u}$ of unambiguous $\pi^+\pi^-\gamma$ decays, where

$$n_{\gamma u} = (2.56\times10^{-3}) \frac{\epsilon_{\gamma u}}{\epsilon_{2\pi}} n_{2\pi} = 7.6 \text{ events.} \qquad (71)$$

The background of leptonic decays in this sample should be less than 0.3 events. In fact, we find 10 events which are unambiguous, according to the above criteria. Both their centre-of-mass photon momentum and decay time distributions are in good agreement with those of simulated $K_S \to \pi^+\pi^-\gamma$ decays, generated with the distribution given by Eq. (64) and subjected to the same cuts. These 10 events therefore provide additional experimental support for our hypothesis that $\pi^+\pi^-\gamma$ decay occurs only through inner bremsstrahlung of the mode $K_S \to \pi^+\pi^-$. They give a value for the decay rate for $k > 50$ MeV/c:

$$\Gamma(K_S \to \pi^+\pi^-\gamma;\ k > 50 \text{ MeV/c}) = (3.3\pm1.2)\times10^{-3}\Gamma(K_S \to \pi^+\pi^-), \qquad (72)$$

which is in agreement with the prediction given in Eq. (68). The error includes an estimated 20 $^{o}/_{o}$ uncertainty in $\epsilon_{\gamma u}$.

It might be thought that we should reduce the $\pi^+\pi^-\gamma$ background as much possible, by removing the unambiguous $\pi^+\pi^-\gamma$ decays and correcting only for the predicted 23.8 ambiguous events. However, as we mentioned in Section IIIE, we find from simulated events that the resolution of the $\pi\mu\nu$ and $\pi\pi\gamma$ hypotheses improves with increasing distance between the production and decay vertices. As a consequence, the time

distribution of unambiguous $\pi^+\pi^-\gamma$ decays is not simply a K_S distribution corrected for geometrical losses; there is an additional depletion at short times, due to the time-dependence of the resolution. To correct our leptonic decay time distributions for a background of ambiguous decays alone, we should have to understand this time-dependent resolution in detail. Instead, we choose to retain also the unambiguous $\pi^+\pi^-\gamma$ decays; the resolution is then irrelevant, and we need apply only geometrical corrections to the expected K_S distribution of the background.

B. Maximum-likelihood Analysis.

The histograms in Figs. 4, 5, and 6 show the time distributions of the positive leptonic, negative leptonic, and ambiguous decays in the interval from 0 to 10^{-9} sec. There were in additional 12 decays at times greater than 10^{-9} sec. We have made a maximum-likelihood analysis of the electronic, muonic, and ambiguous decay time distributions in terms of the parameters x and x' defined in Section II. In this analysis we have used events at all decay times, but our results are in fact completely insensitive to the distribution of the 12 events not shown in the histograms. The solid and broken curves in Figs. 4, 5, and 6 are explained in Section IVC.

Consider first the identified electronic decays. The likelihood of a given value of x, $\mathcal{L}_e(x)$, is simply the probability that, if x truly had this value, the distributions of these events would be as we observed them. Let us expand the notation of Eq. (17), and write the time distribution, predicted by this value of x, of decays with electron charge q, as $\Gamma_e(x; q, t)$. Suppose that in the i-th event we looked at an inter-

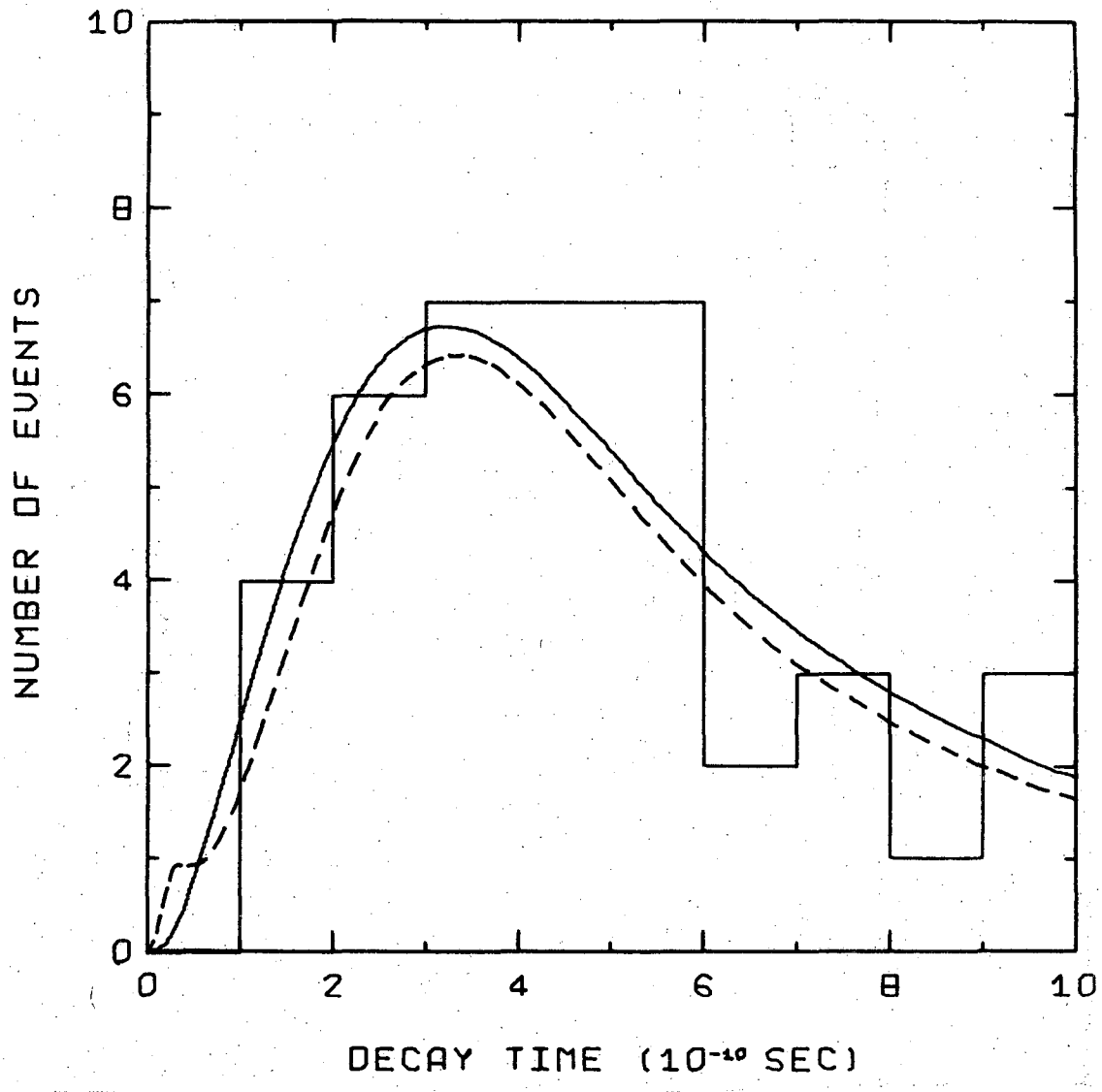

Fig. 4. Time distribution of the 46 positive leptonic decays. The solid and broken curves show the predictions for x=o and x=0.25, and their integrals over the first time bin are 0.92 and 0.90, respectively.

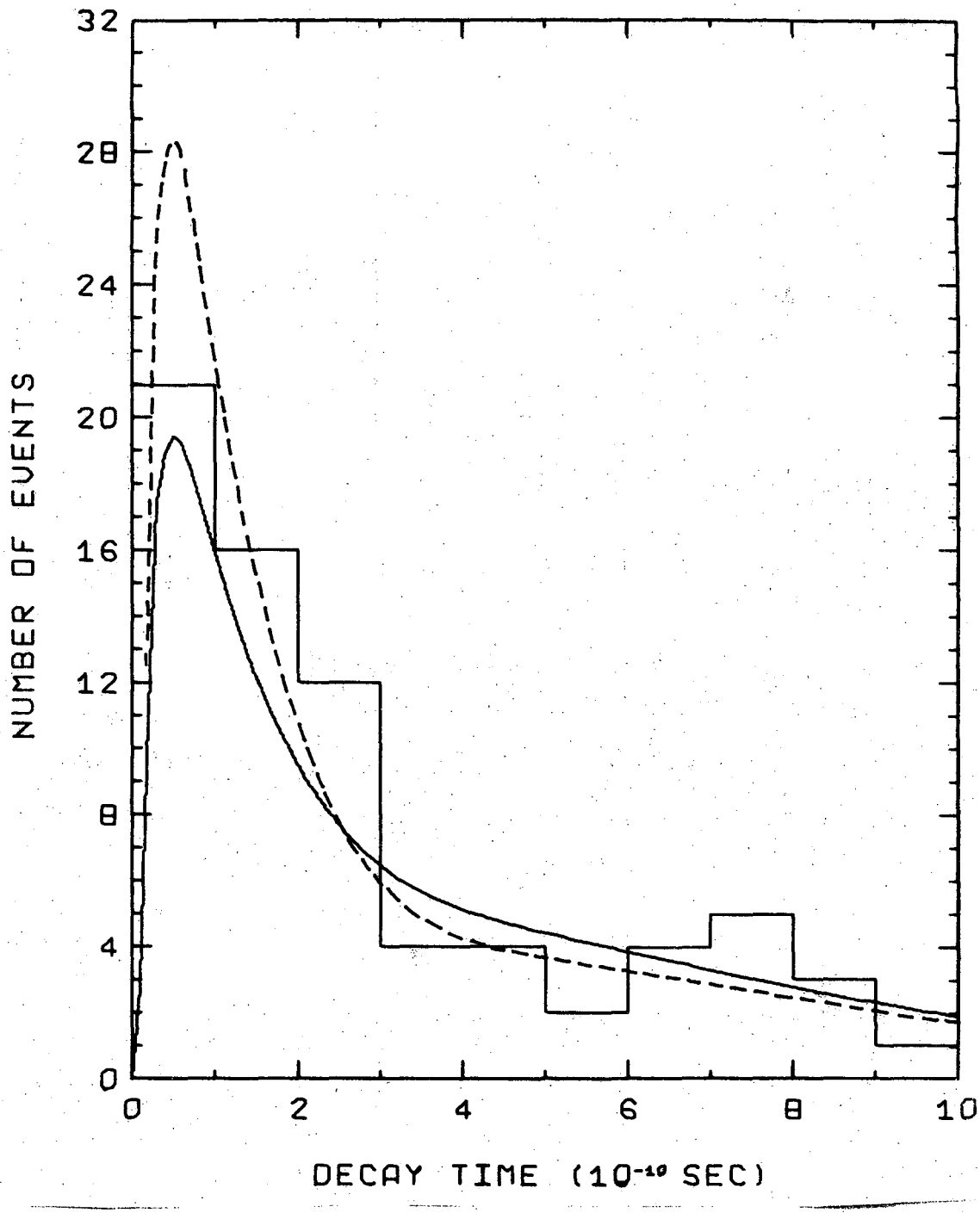

Fig. 5. Time distribution of the 73 negative leptonic decays. The solid and broken curves show the predictions for x=o and x=0.25, and their integrals over the first time bin are 15.0 and 21.6, respectively.

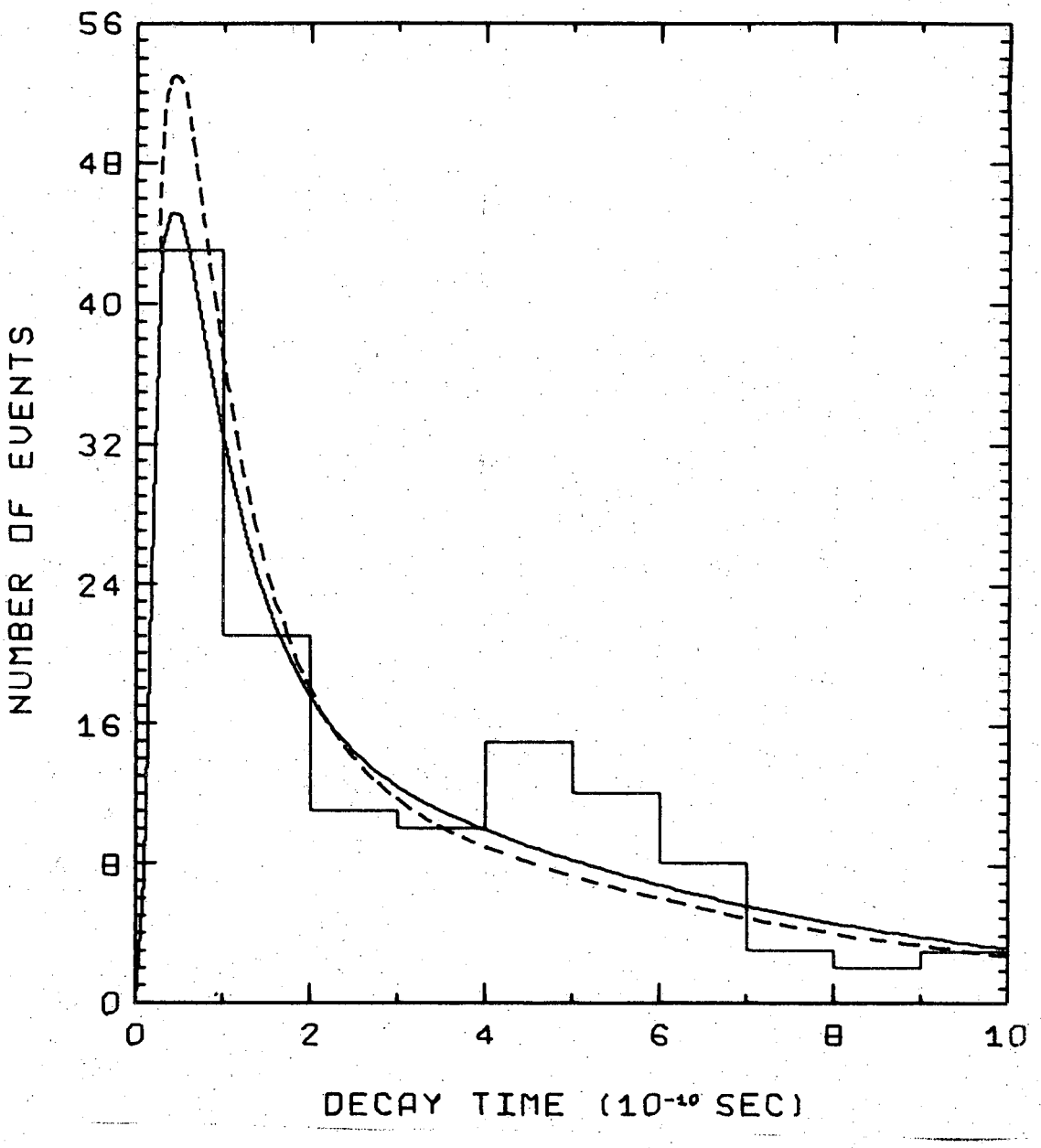

Fig. 6. Time distribution of the 133 unidentified events. The solid and broken curves show the predictions for x=o and x=0.25, and their integrals over the first time bin are 34.1 and 39.5, respectively.

val of time from t^i_{min} to t^i_{max}, and observed a decay with electron charge q^i at time t^i. For every event in our sample, the uncertainty in the decay time is less than 12 $^o/_o$, and we neglect it. First, given that the electron had charge q^i, the differential probability that the decay should occur at time t^i is

$$\frac{\Gamma_e(x;\, q^i,t^i)}{\int_{t^i_{min}}^{t^i_{max}} \Gamma_e(x;q^i,t\,)dt}\,, \tag{73}$$

which is normalized to the interval t^i_{min} to t^i_{max} (with constant detection efficiency) since the decay was actually observed in this interval. Furthermore, the probability that the electron should have charge q^i, rather than $-q^i$, in a decay in this interval, is

$$\frac{\int_{t^i_{min}}^{t^i_{max}} \Gamma_e(x;q^i,t\,)dt}{\int_{t^i_{min}}^{t^i_{max}} \left[\Gamma_e(x;+1,t\,) + \Gamma_e(x;\,-1,t)\right] dt}\,, \tag{74}$$

since our selection and identification procedures are charge-symmetric. The likelihood function is then the product of these two factors for every identified electronic decay:

$$\mathcal{L}_e(x) = \prod_{i=1}^{81} \frac{\Gamma_e(x;\, q^i,t^i)}{\int_{t^i_{min}}^{t^i_{max}} \left[\Gamma_e(x;\,+1,t) + \Gamma_e(x;\,-1,t)\right] dt} \tag{75}$$

A contour plot of this function in the x complex plane is shown in Fig. 7. We have drawn contours at likelihood values $\exp(-\frac{1}{2}n^2)$ relative to the likelihood peak, for n=1, 2, 3, 4, and 5. The location of the peak is shown by the solid circle. If the errors in Re(x) and Im(x) were Gaussian and uncorrelated, the contours shown would be right ellipses of constant separation, representing numbers of standard deviations from the peak. We see that this is approximately the case for small n, so our result for the 81 identified electronic decays may be written:

$$\mathrm{Re}(x) = 0.30\ ^{+0.10}_{-0.12}\ , \quad \mathrm{Im}(x) = 0.07\ ^{+0.10}_{-0.08}, \tag{76}$$

where the errors in Re(x) and Im(x) are essentially uncorrelated and represent one standard deviation limits.

We treated the identified muonic decays in the same way, defining the likelihood function for x' as

$$\mathcal{L}_\mu(x') = \prod_{i=1}^{38} \frac{\Gamma_\mu(x';\ q^i, t^i)}{\int_{t^i_{min}}^{t^i_{max}} \left[\Gamma_\mu(x';\ +1, t) + \Gamma_\mu(x';\ -1, t)\right] dt}, \tag{77}$$

where $\Gamma_\mu(x';\ q,\ t)$ is the time-dependent rate of decay for muon charge q, given by Eqs. (17) and (46). A contour plot of this likelihood function is shown in Fig. 8, and gives as our result for the 38 identified muonic decays:

$$\mathrm{Re}(x') = 0.19\ ^{+0.13}_{-0.18}\ , \quad \mathrm{Im}(x') = -\ 0.12\ ^{+0.20}_{-0.17}\ . \tag{78}$$

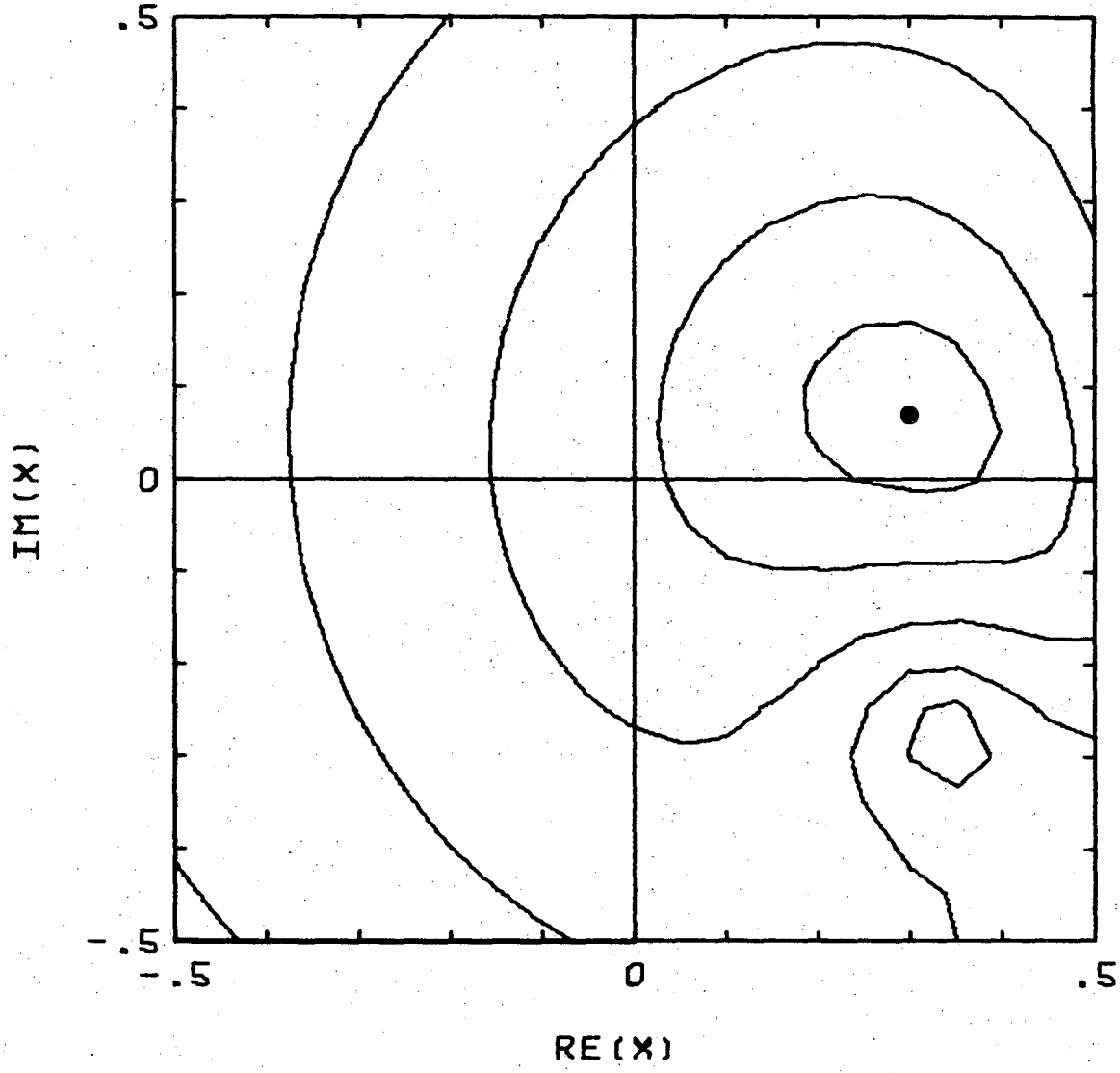

Fig. 7. Likelihood contours for the 81 identified electronic decays.

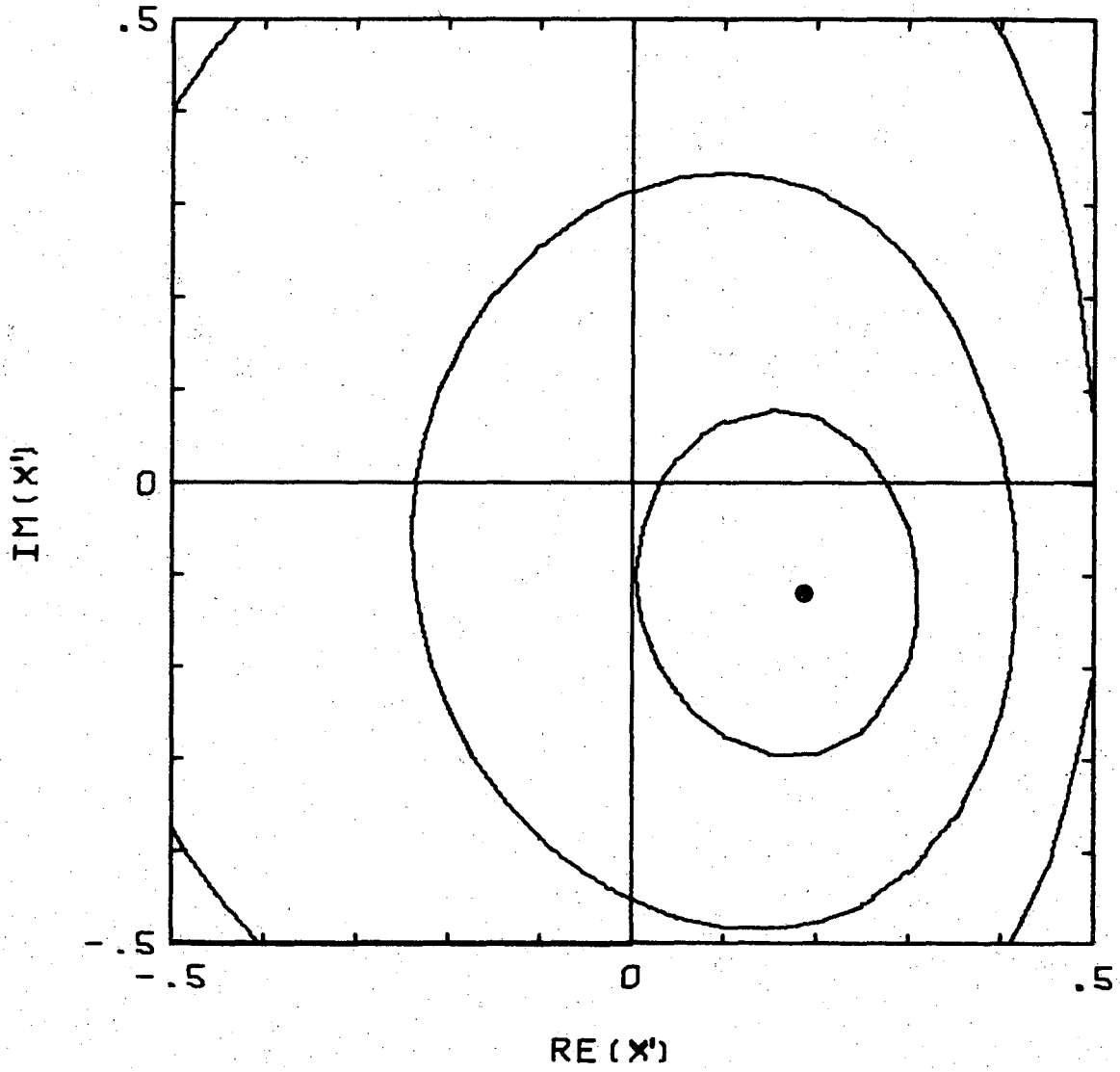

Fig. 8. Likelihood contours for the 38 identified muonic decays.

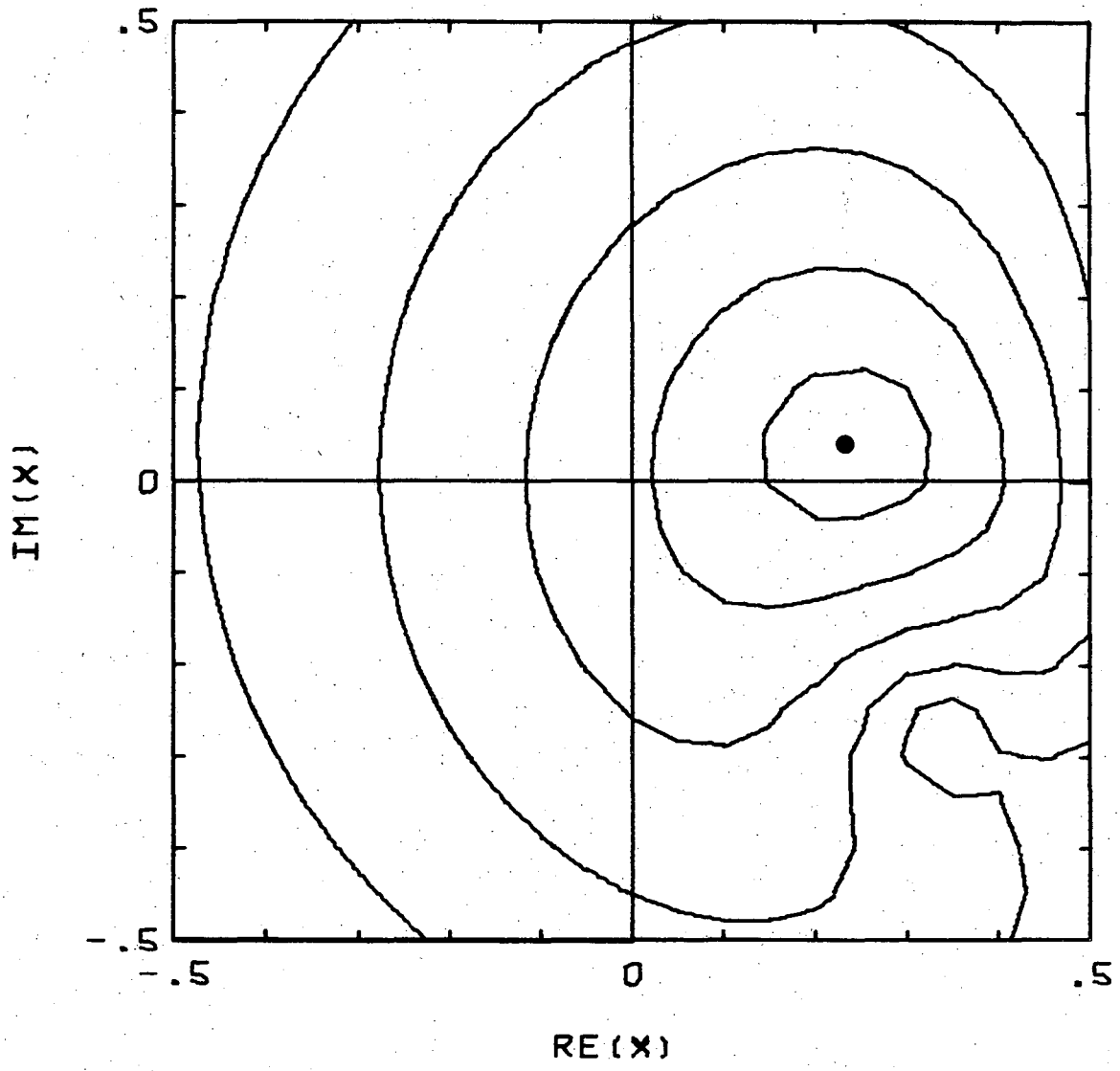

Fig. 9. Likelihood contours for the 119 identified leptonic decays. This likelihood function is the product of those in Figs. 7 and 8.

As in our result (76) for the electronic decays, the errors in (78) are essentially uncorrelated and are one standard deviation limits.

The results (76) and (78) are clearly consistent with the hypothesis $x=x'$, which corresponds to a negligible contribution of the induced scalar interaction in both the electronic and the muonic decay modes. If we make this hypothesis, then both (76) and (78) may be regarded as measurements of the parameter x, and we may combine them to obtain the likelihood contours shown in Fig. 9, which give

$$\mathrm{Re}(x) = 0.23 \pm 0.09 \ , \quad \mathrm{Im}(x) = 0.04 \pm 0.08 \ , \tag{79}$$

from the 119 identified leptonic decays.

The hypothesis that x and x' are equal also allows us to use the ambiguous events to measure their common value. For in this case the electronic and muonic decay rates are proportional at all times:

$$\Gamma_e(x;\, q,\, t) = I_e\, P(x;\, q,t), \quad \Gamma_\mu(x;\, q,\, t) = I'_\mu P(x;\, q,t) \tag{80}$$

where I_e and I'_μ are given by Eq. (39) and (47), and

$$P(x;\, q,t) = |1+x|^2 \exp(-\lambda_S t) + |1-x|^2 \exp(-\lambda_L t) - 2\Big[2\,\mathrm{Im}(x) \sin \delta t + (-1)^q (1-|x|^2) \cos \delta t\Big] \exp\{-\tfrac{1}{2}(\lambda_S + \lambda_L)t\} \ . \tag{81}$$

Since our sample of 133 ambiguous events is expected to contain 31.4 $\pi^+\pi^-\gamma$ decays, as discussed in Section IVA, we apply a correction for these background events in the likelihood function. The corrected function is calculated as follows. Let ϵ_γ represent our detection efficiency for $\pi^+\pi^-\gamma$ decays, in those time intervals where this is independent of time. The detection efficiencies for leptonic decays are incorporated in the integrals I_e and I_μ'; let r_e and r_μ represent the efficiencies for identifying the lepton in these events.

Then, in the time intervals where all the efficiencies are independent of time, the observed rate of ambiguous decays is

$$\Gamma_o(x;t) = \left[(1-r_e)I_e + (1-r_\mu)I'_\mu\right]\left[P(x;+1,t) + P(x;-1,t)\right] + \tfrac{1}{2}\epsilon_\gamma \Gamma(K_S \to \pi^+\pi^-\gamma)\exp(-\lambda_S t). \quad (82)$$

Thus the likelihood function for the ambiguous events, when for the i-th such event the decay time is t^i and the appropriate time interval is from t^i_{min} to t^i_{max}, is[30]

$$\mathcal{L}_o(x) = \prod_{i=1}^{133} \frac{P(x;+1,t^i) + P(x;-1,t^i) + f(x)\exp(-\lambda_S t^i)}{\int_{t^i_{min}}^{t^i_{max}} \left[P(x;+1,t) + P(x;-1,t) + f(x)\exp(-\lambda_S t)\right] dt}, \quad (83)$$

where

$$f(x) = \frac{\tfrac{1}{2}\epsilon_\gamma \Gamma(K_S \to \pi^+\pi^-\gamma)}{(1-r_e)I_e + (1-r_\mu)I'_\mu}.$$

To relate the $\pi^+\pi^-\gamma$ correction factor f(x) to the expected number n_γ (= 31.4) of observed $\pi\pi\gamma$ decays, we note that this number is given by

$$n_\gamma = \tfrac{1}{2}\epsilon_\gamma \Gamma(K_S \to \pi^+\pi^-\gamma)\sum_{\overline{K}^o}\int_{t^i_{min}}^{t^i_{max}} \exp(-\lambda_S t)\, dt. \quad (84)$$

If we define the geometrical efficiency as the function

$$\epsilon(t) = \frac{1}{N}\sum_{\overline{K}^o}\eta_i(t) \quad (85)$$

where N is the number of $\overline{K}^o$'s produced in our fiducial volume and

$$\eta_i(t) = 1 \quad \text{if } t^i_{min} < t < t^i_{max}, \quad (86)$$
$$= 0 \quad \text{otherwise,}$$

then we may write

$$n_\gamma = \frac{N}{2}\epsilon_\gamma \Gamma(K_S \to \pi^+\pi^-\gamma)\int_o^\infty \exp(-\lambda_S t)\,\epsilon(t)\, dt. \quad (87)$$

Similarly the number of leptonic decays in our sample of ambiguous events is

$$n_o - n_\gamma = N\left[(1-r_e)I_e + (1-r_\mu)I'_\mu\right]\int_o^\infty \left[P(x;+1,t) + P(x;-1,t)\right]\epsilon(t)\,dt\,, \quad (88)$$

where n_o is the total number of ambiguous events (= 133). Thus

$$f(x) = \frac{n_\gamma}{n_o - n_\gamma}\,\frac{\int_o^\infty [P(x;+1,t) + P(x;-1,t)]\;\epsilon(t)\,dt}{\int_o^\infty \exp(-\lambda_S t)\;\epsilon(t)\,dt} \equiv \frac{n_\gamma Q(x)}{n_o - n_\gamma}\,. \quad (89)$$

We cannot evaluate the sum in Eq. (85) directly, because we do not in fact observe all $\overline{K}^o$'s, but only those that have a visible decay. However, we can replace the sum over all $\overline{K}^o$'s by a weighted sum over observed $\pi^+\pi^-$ decays, where the weight for each event is the inverse of the probability that a $\overline{K}^o$ produced with that momentum and direction would give an observed $\pi^+\pi^-$ decay. This probability is

$$p_i = \tfrac{1}{2}\,\epsilon_{2\pi}\,\Gamma(K_S \to \pi^+\pi^-)\int_{t^i_{min}}^{t^i_{max}} \exp(-\lambda_S t)\,dt, \quad (90)$$

where $\epsilon_{2\pi}$ is the constant detection efficiency for $\pi^+\pi^-$ decays in the interval from t^i_{min} to t^i_{max}, so

$$\epsilon(t) = \frac{\sum_{\pi^+\pi^-} \eta_i(t)\, p_i^{-1}}{\sum_{\pi^+\pi^-} p_i^{-1}}\,. \quad (91)$$

This function is shown in Fig. 10. We may now perform the integrations in Eq. (89), to find

$$Q(x) = 2\left[\,|1+x|^2 + 12.3\,|1-x|^2 + 5.0\,\mathrm{Im}(x)\,\right], \quad (92)$$

and

$$f(x) = 0.62\,|1+x|^2 + 7.59\,|1-x|^2 + 3.09\,\mathrm{Im}(x). \quad (93)$$

Using this correction in the likelihood function (83), we obtain from the 133 ambiguous events the result

$$\mathrm{Re}(x) = 0.32 \pm 0.12\,, \quad \mathrm{Im}(x) = -0.27^{+0.17}_{-0.20}\,. \quad (94)$$

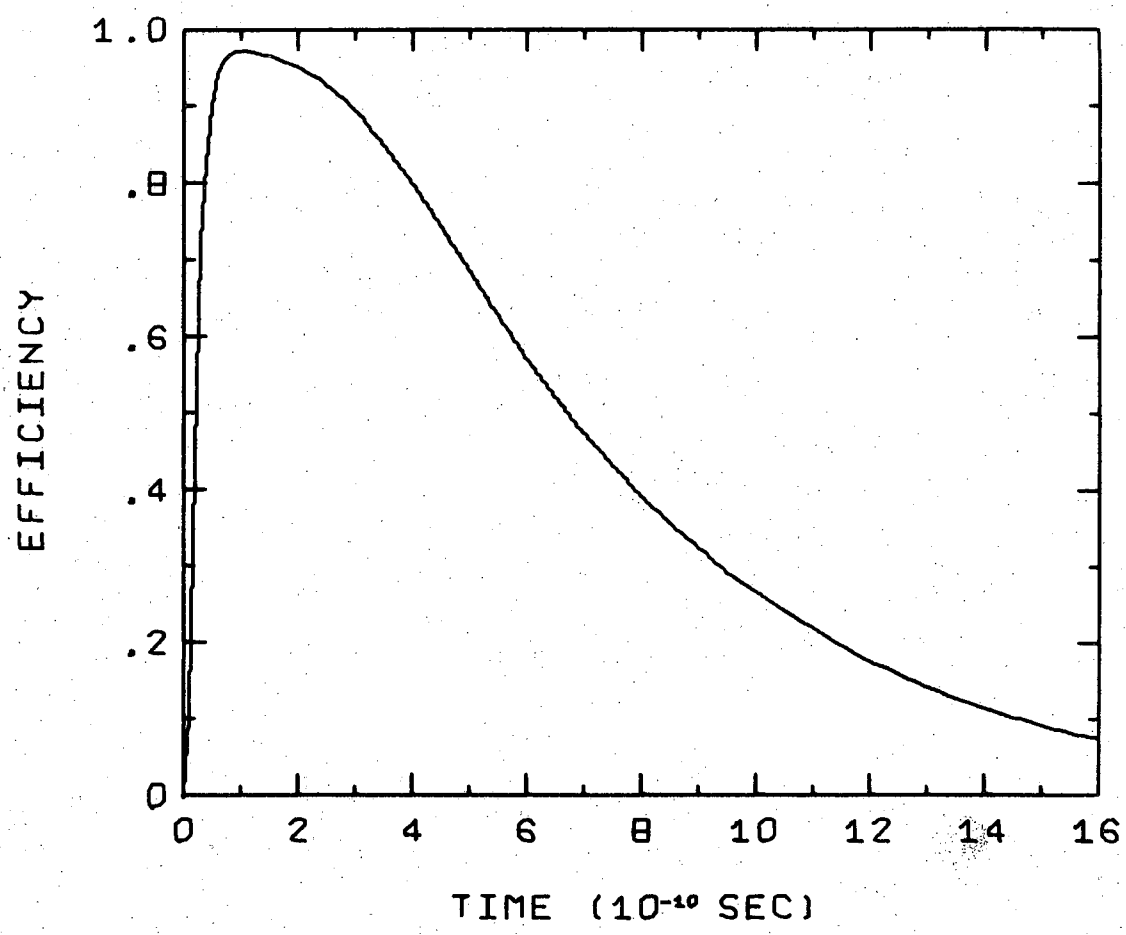

Fig. 10. Geometrical efficiency function.

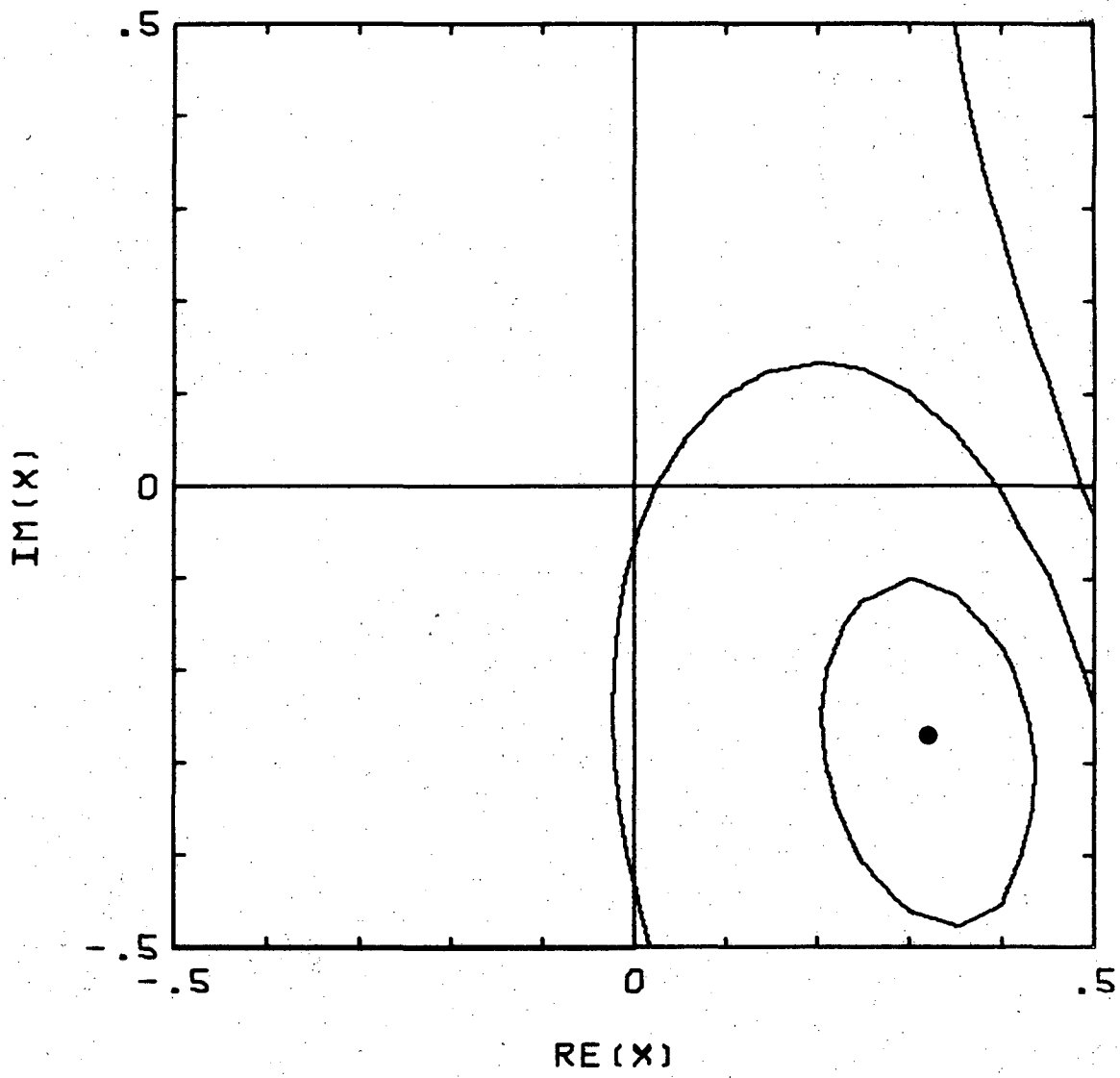

Fig. 11. Likelihood contours for the 133 unidentified events.

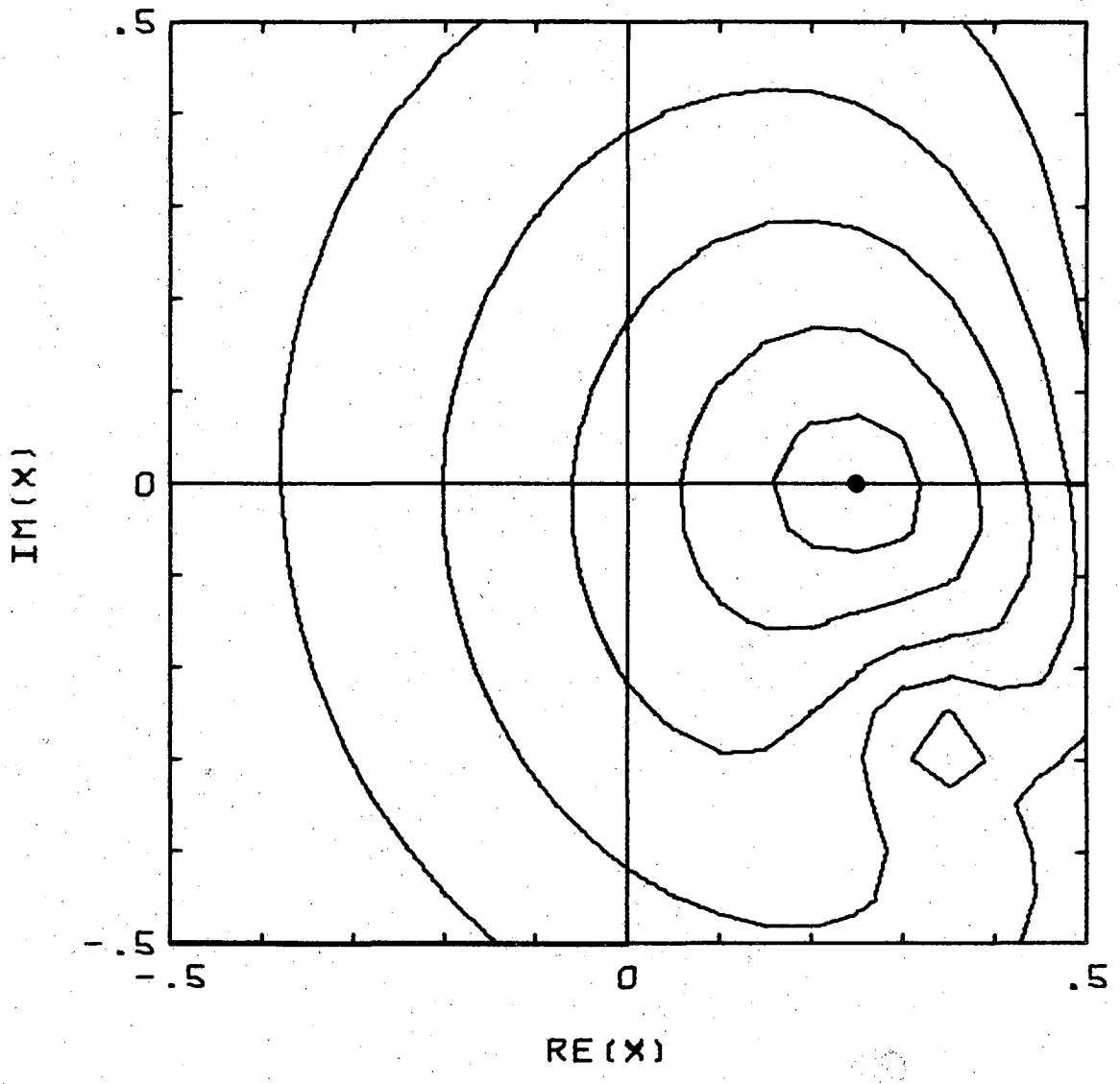

Fig. 12. Likelihood contours for all 252 events. This likelihood function is the product of those in Figs. 9 and 11.

A contour plot of the likelihood is shown in Fig. 11. Combining this likelihood with those for the identified events, we obtain the plot in Fig. 12. The corresponding value of x, determined from all 252 events, is

$$\mathrm{Re}(x) = 0.25^{+0.07}_{-0.09},\ \mathrm{Im}(x) = 0.00 \pm 0.08 \quad . \tag{95}$$

We stress again that this result, unlike (76) and (78), is meaningful only if $x = x'$, that is, only if the induced scalar and pseudoscalar interactions make negligible contributions in both the electronic and the muonic decays. This is not well established, but the results for our identified events are consistent with this hypothesis.

C. Consistency Tests.

A maximum-likelihood analysis gives the relative likelihood of various values of the parameters being measured, but does not indicate whether any of these values gives a good fit to the data. If the parametrization of the time distributions in terms of x is entirely inappropriate, then even our most likely value of x, given by Eq. (95), will give a bad fit to these distributions. We investigated this possibility by making the following three tests of the consistency of our data with the parametrization used.

1. χ^2 test of the time distributions.

The predicted time distributions of the positive leptonic, negative leptonic, and unidentified decays are, respectively,

$$\begin{aligned} \frac{dn}{dt}_+ (x;\, t) &= N_i\, P\,(x;\, +1,\, t)\, \epsilon\,(t), \\ \frac{dn}{dt}_- (x;\, t) &= N_i\, P\,(x;\, -1,\, t)\, \epsilon\,(t), \\ \frac{dn}{dt}_o (x;\, t) &= N_u \left[P\,(x;\, +1,\, t) + P(x;\, -1,\, t) + f(x)\, \exp(-\lambda_S t) \right] \epsilon(t), \end{aligned} \tag{96}$$

where $\epsilon(t)$ is the geometrical efficiency, shown in Fig. 10, and N_i and N_u are normalization constants. We normalize to the observed numbers of identified and unidentified events; since the selection and identification procedures were charge-symmetric, we use the same normalization constant N_i for the positive and negative leptonic distributions. The predictions for x=0 ($\Delta S = \Delta Q$) and x given by Eq. (95) are shown in Figs. 4, 5, and 6 by the solid and broken curves, respectively.

For the ten decay time bins shown in the three distributions, the overall values of χ^2 were 27.0 for the $\Delta S = \Delta Q$ prediction and 26.1 for our result (95). The expectation values of χ^2 were, respectively, 28 (30 bins and 2 normalizations) and 26 (2 independent free parameters). We conclude that, over the time interval from 0 to 10^{-9} sec, both curves give satisfactory fits to the data. We did not use decay times greater than 10^{-9} sec in the χ^2 test, since these bins would contain too few events to give meaningful χ^2 contributions. Even in the interval used, some of the bins contain only one or two events, and the χ^2 provides only a rough test of consistency which is rather insensitive to the parameter x. Of course, these criticisms do not apply to a maximum-likelihood analysis, and for this we used events at all decay times. However, we found that our results were in fact insensitive to the distribution of events beyond 4×10^{-10} sec. For the interval from 0 to 4×10^{-10} sec, in which the statistics are best and the χ^2 should be most sensitive to x, we found χ^2 contributions of 10.8 and 5.3 for $\Delta S = \Delta Q$ and our result (95), respectively, reflecting the greater likelihood of the latter value.

We conclude that the χ^2 test shows a parametrization in terms of x to be appropriate, and is consistent with our likelihood analysis.

2. Measurement of the K_L leptonic decay rate.

Although our analysis of the decay time distributions was independent of the normalization constants N_i and N_u, it was necessary to check the values of these quantities for unexplained losses of events, which might be time-dependent and thus give rise to incorrect results. The only previously well measured quantity with which we may compare our normalization is the leptonic decay rate of the K_L, $\Gamma_L(\ell)$. Noting that

$$P(x; \pm 1, t) = |1 - x|^2 \quad \text{when } \lambda_S^{-1} \ll t \ll \lambda_L^{-1}, \tag{97}$$

we have an observed leptonic decay rate of

$$2(N_i + N_u)|1-x|^2 \epsilon(t) = \tfrac{1}{2} N \epsilon_\ell \epsilon(t) \Gamma_L(\ell) \text{ for } \lambda_S^{-1} \ll t \ll \lambda_L^{-1}, \tag{98}$$

where N is the number of $\overline{K}^o$'s produced in our fiducial volume and ϵ_ℓ is the time-independent part of our detection efficiency for leptonic decays. The total number of leptonic decays seen is

$$\begin{aligned} n_\ell &= (N_i + N_u) \int_o^\infty \left[P(x; +1, t) + P(x; -1, t)\right] \epsilon(t)\, dt, \qquad (99) \\ &= \tfrac{1}{2} N \epsilon_\ell \Gamma_L(\ell) \frac{1}{2|1-x|^2} \int_o^\infty \left[P(x; +1, t) + P(x; -1, t)\right] \epsilon(t) dt. \end{aligned}$$

We calculate N, the number of $\overline{K}^o$'s, from the observed number $n_{2\pi}$ of $K_S \to \pi^+\pi^-$ decays; we have

$$n_{2\pi} = \tfrac{1}{2} N \epsilon_{2\pi} \Gamma(K_S \to \pi^+\pi^-) \int_o^\infty \exp(-\lambda_S t) \epsilon(t)\, dt, \tag{100}$$

where $\epsilon_{2\pi}$ is the time-independent part of the detection efficiency for $\pi^+\pi^-$ decays. This gives

$$\Gamma_L(\ell) = 2 \frac{\epsilon_{2\pi}}{\epsilon_\ell} \frac{n_\ell}{n_{2\pi}} |1-x|^2 [Q(x)]^{-1} \Gamma(K_S \to \pi^+\pi^-), \tag{101}$$

where Q(x) is the ratio of integrals, evaluated in Section IVB:

$$Q(x) = 2\left[|1 + x|^2 + 12.3|1-x|^2 + 5.0\, \mathrm{Im}(x)\right]. \tag{92}$$

In order to evaluate accurately the efficiency ϵ_ℓ by means of the Monte Carlo program PHONY, we had to modify some of our cuts to remove their dependence on qualitative scanning information. For example, in the set of cuts for the test of $\Delta S = \Delta Q$, in which it was not necessary to know ϵ_ℓ, we rejected an event in which the V fit an incoming muon or charged pion decay only when its appearance (ionization, energy-loss, delta-rays, etc.) was consistent with this interpretation. In our cuts for the calculation of the K_L leptonic decay rate, since PHONY could not be made to simulate such complicated criteria, we simply rejected all events satisfying the kinematic criteria for this cut, independent of appearance. Because of these and other similar changes, only 205 of our 252 events were used for the calculation of $\Gamma_L(\ell)$, and the efficiency ϵ_ℓ was found from simulated events to be 41 $^o/_o$. The predicted contamination of $\pi^+\pi^-\gamma$ decays was 27.3 events, so that n_ℓ = 177.7 events.

The determination of $n_{2\pi}$ and $\epsilon_{2\pi}$ was discussed in Section IVA.

It may be seen from Eq. (101) that our measurement of $\Gamma_L(\ell)$ depends on the value assumed for x. This is essentially because the total number of leptonic decays, n_ℓ, enters into the right-hand side of Eq. (101), and the fraction of these that is due to K_L decay depends on the value of x. For x=0, we find $\Gamma_L(\ell) = (13.1\pm1.3)\times 10^6 \text{sec}^{-1}$ and for x= 0.25, $\Gamma_L(\ell) = (11.5\pm1.1)\times10^6$ sec.$^{-1}$ These values may be compared with the current world average,[20] $\Gamma_L(\ell) = (12.24\pm0.46) \times 10^6 \text{sec}^{-1}$. Clearly, this test shows no sign of unexplained loss of events in our experiment. Like the χ^2 test, this test is rather insensitive to x, and gives consistent results for both x= 0 and the value found in the

maximum-likelihood analysis.

3. Measurement of the K_S-K_L mass difference.

To make a more detailed check of the time distributions than is provided by the χ^2 test and the measurement of $\Gamma_L(\ell)$, we made a maximum-likelihood determination of the mass difference δ. We used the likelihood function for all 252 events (assuming x=x', as discussed in Section IVB), allowing δ to vary first instead of, and then in addition to, x. For fixed, real values of x, this function is insensitive to the sign of δ, since the terms involving sin δt in the time distributions vanish when Im(x)=0.

For x fixed at the value zero, as predicted by the $\Delta S = \Delta Q$ rule, we find $|\delta| = (0.47^{+0.12}_{-0.16}) \times 10^{10}$ sec^{-1}. For x=0.25, we obtain $|\delta| = (0.56^{+0.09}_{-0.08}) \times 10^{10}$ sec^{-1}. These values are to be compared with the current world average value[20] of $\delta = (-0.544 \pm 0.017) \times 10^{10}$ sec^{-1}. In both cases, the agreement is very good.

As a final check, we have allowed both x and δ to vary, and have made a simultaneous maximum-likelihood fit to the three quantities Re(x), Im(x), and δ. Here the signs of Im(x) and δ are not determined, but they are coupled, since the likelihood function is invariant under a change of the signs of Im(x) and δ together. Choosing the well established negative sign for δ, we find

$$\mathrm{Re}(x) = 0.25^{+0.08}_{-0.10}\ , \quad \mathrm{Im}(x) = -0.01^{+0.17}_{-0.11}\ , \qquad (102)$$

$$\delta = (-0.56^{+0.15}_{-0.10}) \times 10^{10}\ \text{sec}^{-1}\ .$$

It may be seen that the value of x is essentially unchanged by this procedure, and the agreement of δ with the established value remains

excellent. The small increases in the errors in x, compared with those in Eq. (95), reflect the insensitivity of our result (95) to the value used for δ. More precisely, a change in $|\delta|$ of three "world average standard deviations,"[20] $\Delta|\delta| = \pm 0.05 \times 10^{10}\,\mathrm{sec}^{-1}$, produces a change in our most likely value of x of

$$\Delta x = \pm 0.007 \mp 0.037 i \ . \qquad (103)$$

V. DISCUSSION

Our result (95) is not in good agreement with the prediction of the $\Delta S = \Delta Q$ rule. The likelihood of x=0, relative to the likelihood maximum, is $e^{-3.2} = 0.04$. Alternatively, we may say that the most likely value of x lies about $(2x3.2)^{\frac{1}{2}} = 2.5$ standard deviations away from zero. While we do not regard a 2.5 standard deviation effect as statistically conclusive, it does constitute a strong indication of violation of the $\Delta S = \Delta Q$ rule.

The value we obtain for Im(x) is consistent with zero; thus we find no evidence for a CP-nonconserving contribution to x. However, the limits which we are able to place on Im(x) do not suffice to rule out with certainty the Sachs model of CP violation. This point is discussed in detail in Appendix A.

It may be seen from the curves in Figs. 4, 5, and 6 that our positive result for Re(x) is due mainly to an excess of about 14 negative leptons in the first $3x10^{-10}$ sec, and partly to an excess of about 9 unidentified events in the first 10^{-10} sec. as would result if we had not eliminated all $K_S \rightarrow \pi^+\pi^-$ background. Accordingly we have tried increasing the severity of the cuts (a) to (f) in Section IIID, both one at a time and in various combinations, so as to remove each time about 25 additional events from our sample. These removals have no significant effect on our results, and we are convinced that we have negligible $K_S \rightarrow \pi^+\pi^-$ background. Furthermore, the likelihood plots in Figs. 7 and 12 show that our measurement of x is dominated by the identified electronic decays; the muonic and unidentified events add relatively little information, owing to poor statistics in one case and insensitivity to x in the other. Thus our result (95) is principally based on

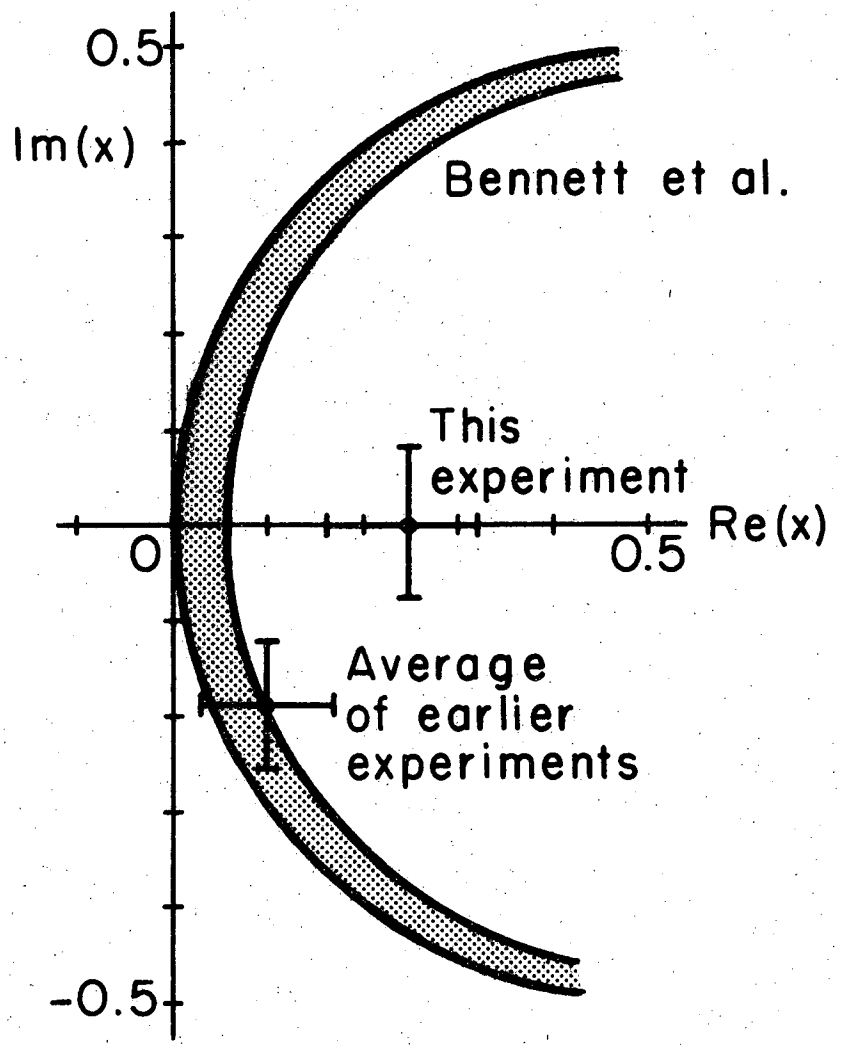

Fig. 13. Experimental results on the value of x.

the set of events that is least likely to be subject to $K_S \to \pi^+\pi^-$ background contamination.

Fig. 13 shows our result for x, together with an average of the results of earlier experiments.[21] The agreement is only fair: the value of χ^2 is 4.7 for two degrees of freedom, giving a confidence level of about 0.1 for consistency of the two values. Nevertheless, the results are in good enough agreement to suggest strongly that x is not zero.

In Fig. 13 we also show the result of a recent experiment,[22] in which the quantity

$$R = \frac{1 - |x|^2}{|1 - x|^2} \tag{104}$$

was determined by analysis of the time-dependent charge asymmetry in electronic neutral K decays. In that experiment, the measured value of R was

$$R = 1.06 \pm 0.06 \ . \tag{105}$$

Curves of constant R are circles in the complex x plane, and the result (105) corresponds to a value of x lying somewhere in the shaded region in Fig. 13. All values of x in this region are in poor agreement with our result, which corresponds to

$$R = 1.67^{+0.27}_{-0.29} \ . \tag{106}$$

Values of x consistent both with earlier experiments and with result (105) are predominantly imaginary, in conflict with our measurement of Im(x). We hope that more accurate determinations of x will soon resolve this conflict.

ACKNOWLEDGMENTS

I am most thankful to Professor Frank S. Crawford, Jr. for his enthusiastic guidance. Many members of the Alvarez Group gave assistance and advice for which I am very grateful. Dr. Margaret Alston-Garnjost and Dr. Frank T. Solmitz made especially valuable contributions. I also wish to thank the 25-inch bubble chamber crew and our scanners and measurers for their help, and Miss Eleanor Kapfenberg for her typing.

It is a great pleasure to acknowledge the interest and support of Professor Luis W. Alvarez.

This work was done under the auspices of the U.S. Atomic Energy Commission, and partly with the support of a N.A.T.O. Research Studentship.

APPENDIX

A. The Sachs Model of CP Violation.

In discussing models of CP violation, it is most convenient to use the "mass matrix" description of the neutral K system, so we begin with an introduction of the mass matrix notation.[23]

If we write the general neutral K state as a column vector,

$$\Psi = \begin{pmatrix} \psi_1 \\ \psi_2 \end{pmatrix} = \psi_1 |K^o\rangle + \psi_2 |\overline{K}^o\rangle \ , \tag{107}$$

then the equation of motion is

$$\frac{d\Psi}{dt} = -iM\Psi \ , \tag{108}$$

where

$$M = \begin{pmatrix} \langle K^o|M|K^o\rangle & \langle K^o|M|\overline{K}^o\rangle \\ \langle \overline{K}^o|M|K^o\rangle & \langle \overline{K}^o|M|\overline{K}^o\rangle \end{pmatrix} . \tag{109}$$

M is called the mass matrix. It is not hermitian, and is often split into its hermitian and anti-hermitian parts:

$$M = M_0 - \tfrac{1}{2}i\Gamma \ , \tag{110}$$

where M_0 and Γ are hermitian. Γ is called the decay matrix, by analogy with the corresponding expressions for a one-dimensional system ϕ :

$$\frac{d\phi}{dt} = -i\mu\phi \ , \tag{111}$$

$$\mu = m - \tfrac{1}{2}i\lambda \ ,$$

where m is the real mass and λ is the decay rate.

We assume that M is CPT-invariant, so that

$$\langle K^o|M|K^o\rangle = \langle \overline{K}^o|M|\overline{K}^o\rangle . \tag{112}$$

A CP-invariant mass matrix would also have

$$\langle \overline{K}^o|M|K^o\rangle = \langle K^o|M|\overline{K}^o\rangle , \tag{113}$$

so we write

$$M = \begin{pmatrix} m & a \\ a+c & m \end{pmatrix} \ , \tag{114}$$

where c ($|c| \ll |a|$) represents a small CP violation.

The independently propagating states K_S and K_L have definite masses and lifetimes, so M is diagonalized by choosing these states as a basis. Thus, if we write

$$|K_{S,L}\rangle = \frac{1}{[2\,(1+|\epsilon|^2)]^{\frac{1}{2}}} \left[(1+\epsilon)\,|K^0\rangle \pm (1-\epsilon)|\overline{K}^0\rangle \right], \quad (115)$$

then $\begin{pmatrix} 1+\epsilon \\ 1-\epsilon \end{pmatrix}$ and $\begin{pmatrix} 1+\epsilon \\ -1+\epsilon \end{pmatrix}$ are the eigenvectors of M, and the corresponding eigenvalues are

$$\mu_\alpha = m_\alpha - \tfrac{1}{2} i\, \lambda_\alpha \qquad (\alpha = S,L) \quad (116)$$

The CP violation parameters c and ϵ may now be related by solving the eignevalue problem for M. We have

$$\begin{vmatrix} m-\mu_\alpha & a \\ a+c & m-\mu_\alpha \end{vmatrix} = 0 ,$$

so $$\mu_\alpha = m \pm \{a\,(a+c)\}^{\frac{1}{2}} ,$$

or, to first order in c/a,

$$\mu_{S,L} = m \pm \tfrac{1}{2}\,(2a + c). \quad (117)$$

Thus $$a(1-\epsilon) = \tfrac{1}{2}\,(2a+c)\,(1+\epsilon) ,$$

giving $$\epsilon = -c/4a , \quad (118)$$

or $$\epsilon = -\frac{c}{2(\mu_S - \mu_L)} , \quad (119)$$

to first order in c/a.

We are now ready to consider the Sachs model.[6] Sachs observed that if the CP violation was confined to mass matrix terms involving leptonic intermediate states, but was large in these terms, then $|\epsilon|$ would have the observed order of magnitude. This is seen as follows. We suppose

$c = \langle \overline{K}^0 | M | K^0 \rangle - \langle K^0 | M | \overline{K}^0 \rangle$ = terms with leptonic intermediate states.

If the leptonic decay parameters x and x' (see p. 15) are roughly equal, we can define suitably averaged decay amplitudes which we denote by

$$f = \langle \pi^- \ell^+ \nu \,|T|\, K^0 \rangle \text{ and } g = \langle \pi^- \ell^+ \nu \,|T|\, \bar{K}^0 \rangle \,. \tag{120}$$

Then by CPT invariance

$$f^* = \langle \pi^+ \ell^- \nu \,|T|\, \bar{K}^0 \rangle \;, \quad g^* = \langle \pi^+ \ell^- \nu \,|T|\, K^0 \rangle \,. \tag{121}$$

Here T represents the decay interaction, and

$$g/f = x \,, \tag{122}$$

so, to lowest order,

$$\lambda^{\ell}_L \equiv \Gamma(K_L \to \pi\, \ell\, \nu) = |f - g|^2 = |f|^2\, |1 - x|^2 \,. \tag{123}$$

Although we do not know precisely how to express c in terms of these amplitudes (because of the usual convergence problems in perturbation theory), we can be confident that

$$\begin{aligned} |c| \sim \big| &\langle \bar{K}^0 | T | \pi^- \ell^+ \nu \rangle \langle \pi^- \ell^+ \nu | T | K^0 \rangle + \langle \bar{K}^0 | T | \pi^+ \ell^- \nu \rangle \langle \pi^+ \ell^- \nu | T | K^0 \rangle \\ &- \langle K^0 | T | \pi^- \ell^+ \nu \rangle \langle \pi^- \ell^+ \nu | T | \bar{K}^0 \rangle - \langle K^0 | T | \pi^+ \ell^- \nu \rangle \langle \pi^+ \ell^- \nu | T | \bar{K}^0 \rangle \big| \\ = \;& 4\, |\mathrm{Im}(f^* g)| \\ = \;& 4\, |f|^2\, |\mathrm{Im}(x)| \,, \end{aligned} \tag{124}$$

so that

$$\begin{aligned} |\epsilon| &\sim 2\, |f|^2\, \frac{|\mathrm{Im}(x)|}{|\mu_S - \mu_L|} \\ &= \frac{2\, \lambda^{\ell}_L}{|\mu_S - \mu_L|}\, \frac{|\mathrm{Im}(x)|}{|1 - x|^2} \,. \end{aligned} \tag{125}$$

Now $$|\mu_S - \mu_L| \cong \tfrac{1}{2} \lambda_S\, |1+i| = \frac{1}{\sqrt{2}}\, \lambda_S \,, \text{ since } m_L - m_S \cong \tfrac{1}{2}\lambda_S, \tag{126}$$

So we conclude

$$\begin{aligned} |\epsilon| &\sim 2\sqrt{2}\, \frac{\lambda^{\ell}_L}{\lambda_S}\, \frac{|\mathrm{Im}(x)|}{|1 - x|^2} \\ &\sim 3 \times 10^{-3}\, \frac{|\mathrm{Im}(x)|}{|1 - x|^2} \,. \end{aligned} \tag{127}$$

In the Sachs model, there is no CP violation in non-leptonic decay processes, so the measured quantity[20]

$$\eta_{+-} = \frac{\langle \pi^+\pi^- | T | K_L \rangle}{\langle \pi^+\pi^- | T | K_S \rangle} = (1.92\pm0.04)\times10^{-3} \exp\{ i(50\pm8) \text{ deg} \} \tag{128}$$

is simply equal to ϵ. Sachs originally proposed that $x \sim \pm i$, for then the prediction (127) would be

$$|\eta_{+-}| = |\epsilon| \sim 1.5\times 10^{-3}, \tag{129}$$

in excellent agreement with experiment. However, our experiment definitely excludes such large values of Im(x), and sets the limit (at the one standard deviation level)

$$\frac{|\text{Im}(x)|}{|1-x|^2} \leq 0.14, \tag{130}$$

This limit restricts the value of $|\eta_{+-}|$ that can be produced by the Sachs mechanism to

$$|\eta_{+-}| = |\epsilon| \lesssim 0.4\times10^{-3}, \tag{131}$$

a prediction that is now in rather poor agreement with (128). In view of its order-of-magnitude nature, though, the prediction (131) is not bad enough to rule out the model with certainty.

Many models of CP violation, including that of Sachs, predict an exact relation between the modulus and phase of ϵ.

This relation is obtained by noting that, although we cannot calculate exact contributions of certain processes to the whole mass matrix M, we can calculate the contributions to the decay matrix Γ. For it follows from unitarity that

$$\langle K^0 | \Gamma | K^0 \rangle = \langle \bar{K}^0 | \Gamma | \bar{K}^0 \rangle = \sum_F \langle K^0 | T | F \rangle \langle F | T | K^0 \rangle \tag{132}$$

and $$\langle \bar{K}^0 | \Gamma | K^0 \rangle = \langle K^0 | \Gamma | \bar{K}^0 \rangle^* = \sum_F \langle \bar{K}^0 | T | F \rangle \langle F | T | K^0 \rangle,$$

where the sum is over all possible decay final states. Now the decay matrix for the mass matrix in Eq. (114) is

$$\mathbf{\Gamma} = \begin{pmatrix} -2\mathrm{Im}(m) & -2\mathrm{Im}(a) - ic^* \\ -2\mathrm{Im}(a) + ic & -2\mathrm{Im}(m) \end{pmatrix} \tag{133}$$

so the CP violation in the decay matrix is

$$\langle \bar{K}^0 | \mathbf{\Gamma} | K^0 \rangle - \langle K^0 | \mathbf{\Gamma} | \bar{K}^0 \rangle = 2i\ \mathrm{Re}(c) \tag{134}$$
$$= g^* f + f\bar{g}^* - f^* g - g f^*$$
$$= -4i\ \mathrm{Im}(f^* g) \text{ in the Sachs model.}$$

But, taking the real part of c from Eq. (119), we have

$$\mathrm{Re}(c) = -2\ \mathrm{Re}\left[(\mu_S - \mu_L)\, \epsilon \right] \tag{135}$$
$$= -2 \left[\delta\ \mathrm{Re}(\epsilon) + \tfrac{1}{2}\ \lambda_S\ \mathrm{Im}(\epsilon) \right] ,$$

where $\delta = m_S - m_L$, and we obtain the relation (136)

$$\delta\ \mathrm{Re}(\epsilon) + \tfrac{1}{2}\ \lambda_S\ \mathrm{Im}(\epsilon) = \mathrm{Im}(f^* g) = \lambda^{\ell}_L\ \frac{\mathrm{Im}(x)}{|1-x|^2} .$$

Using the measured value of $|\eta_{+-}|$, we may obtain from Eq. (136) the Sachs model prediction of the phase of η_{+-}:[31]

$$\arg\ (\eta_{+-}) = \arg\ (\epsilon) = \sin^{-1}\left(\frac{0.8\ \mathrm{Im}(x)}{|1-x|^2} \right) + 43 \text{ deg.} \tag{137}$$

For $x \cong \pm i$, as originally proposed by Sachs, the predictions are

$$\arg\ (\eta_{+-}) = 67 \text{ deg for } x = +i, \tag{138}$$

and $\arg\ (\eta_{+-}) = 19$ deg for $x = -i$.

Both of these are in poor agreement with the measured phase, (50±8) deg. However, for x within the limits set by our experiment, our result (130) and Eq. (137) give

$$36 \text{ deg} \leq \arg\ (\eta_{+-}) \leq 50 \text{ deg} , \tag{139}$$

in good agreement with experiment.

In conclusion we may say that, although our experiment rules out

large values of $|\mathrm{Im}(x)|$, this is not of great interest, as such large values are already excluded on the basis of the phase prediction (137). The limits set on $|\mathrm{Im}(x)|$ by our experiment are almost sufficient to rule out the Sachs model on the basis of the prediction (131) of $|\eta_{+-}|$, but a limit of $|\mathrm{Im}(x)| < 0.04$ will be required to show with certainty that the model is not valid.

In the above discussion, we have not mentioned the quantity

$$\eta_{oo} = \frac{\langle \pi^o\pi^o | T | K_L \rangle}{\langle \pi^o\pi^o | T | K_S \rangle} \tag{140}$$

because experimental results on $|\eta_{oo}|$ are still uncertain. However, the Sachs model clearly predicts $|\eta_{oo}| = |\eta_{+-}| = |\epsilon|$, so the result $|\eta_{oo}| \neq |\eta_{+-}|$ would suffice to disprove the model.

B. The Coulomb Scattering Cut.

The Rutherford cross-section[24] for the Coulomb scattering of a pion on a proton is

$$\frac{d\sigma}{d\Omega} = \left(\frac{e^2}{2pc\beta}\right)^2 \frac{1}{\sin^4 \theta_s/2} , \tag{141}$$

where p is the momentum of the pion, $c\beta$ its velocity, and θ_s the scattering angle. For small angles, this gives

$$\frac{d\sigma}{d\theta_s} = 2\pi \left(\frac{2e^2}{pc\beta}\right)^2 \theta_s^{-3} , \tag{142}$$

which may be written

$$\frac{d\sigma}{d(p\beta\theta_s)} = 2\pi \left(\frac{2e^2}{c}\right)^2 (p\beta\theta_s)^{-3} . \tag{143}$$

Thus the total cross-section for Coulomb scattering with $p\beta\theta_s > F_s$ is

$$\sigma(p\beta\theta_s > F_s) = \pi \left(\frac{2e^2}{c}\right)^2 F_s^{-2} . \tag{144}$$

The fraction of $\pi^+\pi^-$ decays in which a pion scatters with $p\beta\theta_s > F_s$ is given by

$$f = 2\eta\ell \ \sigma(p\beta\theta_s > F_s) = 2\pi\eta\ell \left(\frac{2e^2}{c}\right)^2 F_s^{-2} , \qquad (145)$$

where $\eta = 3\text{x}10^{22}$ is the number of protons per cc in the bubble chamber and ℓ is the average measured pion track length. The factor of two occurs because there are two pions per event.

It is clear that a Coulomb scattering at the end of a measured track segment will have no effect on the measured direction of the track, while such a scattering near the beginning of the track will give a direction which is incorrect by the angle of scattering, θ_s. For scattering at intermediate points, the error in the direction of the track is more difficult to calculate; however, it is safe to say that the average error is about $\Delta\theta = \frac{1}{2}\theta_s$. Thus

$$p\beta\Delta\theta \approx \tfrac{1}{2}\, p\beta\theta_s \qquad (146)$$

and the fraction of events with $p\beta\Delta\theta > F$ is

$$f = 2\,\eta\,\ell\ \sigma(p\beta\theta_s > 2F) = 2\pi\eta\ell \left(\frac{e^2}{c}\right)^2 F^{-2} . \qquad (147)$$

Taking ℓ=15 cm and noting that $e^2/c = \alpha\hbar = 4.7\text{x}10^{-24}$ MeV-sec, we find

$$f = 192\ F^{-2} , \qquad (148)$$

where F is expressed in (MeV/c) deg. For F=2 200, this gives

$$f = 4\text{x}10^{-5} \qquad (149)$$

Thus, out of some 13 000 $K_s \to \pi^+\pi^-$ decays that survive our fiducial volume and dip angle cuts, we expect only 0.5 events with a Coulomb scattering such that $p\beta\Delta\theta > 2\,200$ (MeV/c) deg.

Next we consider $\pi \to \mu\,\nu$ decays, which give rise to track direction errors in the same way as Coulomb scattering of the pion.

In the case that the muon is emitted perpendicular to the line of flight of the pion in the latter's rest frame, we have

$$\tan \theta_d = \beta^* / \beta\gamma \ , \tag{150}$$

where θ_d is the decay angle in the laboratory, $\beta^* = 0.27$ is the muon velocity (in unit of c) in the pion rest frame, and $\beta\gamma = pc/m_\pi$, where p is the pion momentum. Thus for all $\pi \to \mu\, \nu$ decays, we have

$$p\beta\Delta\theta \lesssim p\beta\theta_d < p\theta_d < p \tan \theta_d \lesssim \beta^* m_\pi/c = 37.7 \text{ MeV/c} \tag{151}$$

when $\Delta\theta$ is expressed in radians, or

$$p\beta\Delta\theta < 2160 \quad \text{(MeV/c) deg,} \tag{152}$$

and our cut at $p\beta\Delta\theta$ = 2 200 (MeV/c) deg will remove all $\pi \to \mu\, \nu$ decays.

C. The Cut to Remove Second-order Background.

We consider first the expected errors in the measured track quantities when a pion track contains a Coulomb scattering such that $p\beta\Delta\theta = F$. We take the following to be the independent measured quantities characterizing the track: ϕ, the azimuthal angle, s, the dip tangent, and k, the inverse projected momentum. In terms of the dip λ and the momentum p of the track, we have

$$\begin{aligned} s &= \tan \lambda \ , \\ k &= 1/p \cos \lambda \ , \\ \text{so} \qquad p^2 &= \hat{} \ (1 + s^2)/k^2 \ . \end{aligned} \tag{153}$$

The r.m.s. errors in ϕ and s are

$$\begin{aligned} \delta\phi &= \frac{1}{\sqrt{2}} \frac{\Delta\theta}{\cos \lambda} = \frac{1}{\sqrt{2}} pk\, \Delta\theta \\ \text{and} \qquad \delta s &= \frac{1}{\sqrt{2}} \frac{\Delta\theta}{\cos^2 \lambda} = \frac{1}{\sqrt{2}} p^2 k^2\, \Delta\theta \ . \end{aligned} \tag{154}$$

For the momentum measurement, the worst situation occurs when the

scattering lies at the middle of the measured track segment. In

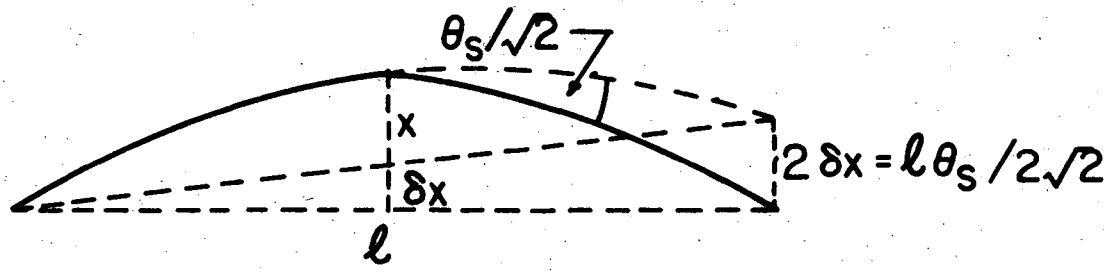

this case, we see from the diagram above that the r.m.s. error in the track sagitta x is

$$\delta x = \frac{1}{4\sqrt{2}} \ell \theta_s \approx \frac{1}{2\sqrt{2}} \ell\Delta\theta, \tag{155}$$

where ℓ is the length of the segment. The sagitta and the inverse projected momentum k are related by the equation

$$x = \frac{3}{80} B \ell^2 k, \tag{156}$$

where B is the magnetic field in kilogauss, so we obtain

$$\delta k = \frac{20\sqrt{2}}{3B\ell} \Delta\theta . \tag{157}$$

Writing $\Delta\theta = p^{-1}\beta^{-1} F$, we obtain for Coulomb scattering

$$\delta\phi_c = \frac{1}{\sqrt{2}} k\beta^{-1} F,$$

$$\delta s_c = \frac{1}{\sqrt{2}} pk^2\beta^{-1} F, \tag{158}$$

and

$$\delta k_c = \frac{20\sqrt{2}}{3B\ell} p^{-1}\beta^{-1} F .$$

Next we consider the emission of two photons of momentum P at the decay vertex. The largest angular errors occur when each pion track is perpendicular to a photon direction in the centre-of-mass

frame; in this case $\Delta\theta \approx P/p$ for both tracks, and

$$\delta\phi_\gamma = \frac{1}{\sqrt{2}} kP \ , \qquad (159)$$

$$\delta s_\gamma = \frac{1}{\sqrt{2}} pk^2 P \ .$$

The largest momentum errors, on the other hand, occur when each pion track is parallel to a photon direction, when $\delta p \approx P$ and

$$\delta k_\gamma = p^{-1} k P \ . \qquad (160)$$

The track reconstruction program TVGP[25] calculates for each track a 6x6 matrix of the measurement errors in the quantities ϕ, s, and k at the beginning and end of the measured track segment. Taking F= 376 (MeV/c) deg = 6.56 (MeV/c) radians and P = 10 MeV/c, we increased the diagonal elements of the error matrices for the two decay tracks before making the fit discussed on p. 30, according to the prescription

$$(\delta\phi_b)^2 \to (\delta\phi_b)^2 + (\max[\delta\phi_c, \delta\phi_\gamma])^2, \ (\delta\phi_e)^2 \to (\delta\phi_e)^2 + (\max[\delta\phi_c, \delta\phi_\gamma])^2 \ , \qquad (161)$$

and similarly for s and k, where the subscripts "b" and "e" denote values at the beginning and end of the track, respectively. Although this prescription is very crude, we believe that it should enable second-order background events to obtain a good value of χ^2 for our special fit, which will lead to their rejection.

REFERENCES

1. R. P. Feynman and M. Gell-Mann, Phys. Rev. 109, 193 (1958).

2. The averages of results prior to our experiment were made by A. H. Rosenfeld, N. Barash-Schmidt, A. Barbaro-Galtieri, L. R. Price, P. Söding, C. G. Wohl, M. Roos, and W. J. Willis, Rev. Mod. Phys. 40, 77 (1968).

3. N. Cabibbo, Phys. Rev. Letters 10, 531 (1963).

4. R. P. Ely, W. M. Powell, H. White, M. Baldo-Ceolin, E. Calimani, S. Ciampolillo, O. Fabbri, F. Farini, C. Filippi, H. Huzita, G. Miari, U. Camerini, W. F. Fry, and S. Natali, Phys. Rev. Letters 8, 132 (1962); G. Alexander, S. P. Almeida, and F. S. Crawford, Jr., ibid. 9, 69 (1962); B. Aubert, L. Behr, F. L. Canavan, L. M. Chounet, J. P. Lowys, P. Mittner, and C. Pascaud, Phys. Letters 17, 59 (1965); M. Baldo-Ceolin, E. Calimani, S. Ciampolillo, C. Filippi-Filosofo, H. Huzita, F. Mattioli, and G. Miari, Nuovo Cimento 38, 684 (1965); P. Franzini, L. Kirsch, P. Schmidt, J. Steinberger, and J. Plano, Phys. Rev. 140, B127 (1965); L. Feldman, S. Frankel, V. L. Highland, T. Sloan, O. B. Van Dyck, W. D. Wales, R. Winston, and D. M. Wolfe, Phys. Rev. 155, 1611 (1967); D. G. Hill, D. Luers, D. K. Robinson, M. Sakitt, O. Skjeggestad, J. Canter, Y. Cho, A. Dralle, A. Engler, H. E. Fisk, R. W. Kraemer, and C. M. Meltzer, Phys. Rev. Letters 19, 668 (1967).

5. Preliminary results of our experiment, based on 242 events, were published by Bryan R. Webber, Frank T. Solmitz, Frank S. Crawford, Jr., and Margaret Alston-Garnjost, Phys. Rev. Letters 21, 498 (1968), and ibid. 21, 715 (1968).

6. R. G. Sachs, Phys. Rev. Letters 13, 286 (1964).

7. A complete review of the phenomenology of neutral K leptonic decays is given by T. D. Lee and C. S. Wu, Ann. Rev. Nucl. Sci. 16, 511 (1966). However, we give here a full discussion of the relevant theory, in order to clarify the assumptions made in the analysis of our data.

8. We use the values $\lambda_S^{-1} = 0.862 \times 10^{-10}$ sec, $\lambda_L^{-1} = 5.38 \times 10^{-8}$ sec, $m_S - m_L = -0.544 \times 10^{10}$ sec^{-1}, from the compilation by the Particle Data Group, Rev. Mod. Phys. 41, 109 (1969).

9. See, for example, J. S. Bell, Theory of Weak Interactions, in High Energy Physics Lectures, Les Houches, 1965 (Gordon and Breach, New York, 1965), p. 471. The theorem concerns the effects of final-state interactions, which, being electromagnetic, are of order α.

10. In fact, there are serious disagreements between the various measured values of this quantity. These disagreements cannot be resolved by assuming a large energy dependence. Traditionally, it is assumed in experiments on K_L decay that x=y=0, and the measured quantity $(\xi+y)/(1+x)$ is assumed to be simply ξ. Data on this quantity are therefore listed as determinations of ξ in the Particle Data Group compilation (Ref. 8).

11. Meson resonances that dominate the form factors will all have $(\text{mass})^2$ much greater than the maximum value of $q^2 = (m_K - m_\pi)^2$, so the energy dependence of all the form factors should be small in the region of physical q^2.

12. Roger O. Bangerter, K-65 Beam Optics, Lawrence Radiation Laboratory Alvarez Group Physics Note 574, Oct. 1965 (unpublished).

13. We thank Dr. A. Engler (Carnegie-Mellon University, Pittsburgh,

Pennsylvania) for calling our attention to this effect in a private communication, 1969.

14. F. T. Solmitz, A. D. Johnson, and T. B. Day, Three View Geometry Program, Lawrence Radiation Laboratory Alvarez Group Programming Note P-117, Oct. 1965 (unpublished).

15. D. Drijard and E. R. Burns, Jr. (Lawrence Radiation Laboratory), private communication, 1967.

16. This criterion was first used by Robert L. Golden, Leptonic Decays of Neutral K Mesons (Ph.D. Thesis), Lawrence Radiation Laboratory Report UCRL-16771, March 1966 (unpublished).

17. Frank S. Crawford, Jr., Use of Delta Rays to Determine Particle Velocities, Lawrence Radiation Laboratory Report UCID-241, Nov. 1957 (unpublished).

18. E. Bellotti, A. Pullia, M. Baldo-Ceolin, E. Calimani, S. Ciampolillo, H. Huzita, F. Mattioli, and A. Sconza, Nuovo Cimento 45A, 737 (1966).

19. This spectrum was first calculated by M. Bég, R. Friedberg, and J. Schultz, as quoted by Franzini et al. (Ref. 4).

20. All the world average values quoted are taken from the Particle Data Group compilation (Ref. 8).

21. The results of the following experiments were used in making the average of earlier determinations of x: Aubert et al. (Ref. 4), Baldo-Ceolin et al. (Ref. 4), Franzini et al. (Ref. 4), Feldman et al. (Ref. 4), and Hill et al. (Ref. 4).

22. S. Bennett, D. Nygren, H. Saal, J. Sunderland, J. Steinberger, and K. Kleinknecht, Phys. Letters 27B, 244 (1968).

23. A more detailed discussion of the phenomenology of the mass matrix is given by J. S. Bell and J. Steinberger, Weak Interactions of Kaons, in Proceedings of the Oxford International Conference on Elementary Particles (Rutherford High Energy Laboratory, Chilton, England, 1966), p. 195.

24. For a quantum-mechanical derivation of Eq. (141) see, for example, M. L. Goldberger and K. M. Watson, Collision Theory (John Wiley and Sons, Inc., New York, 1964), p. 95.

25. Ref. 14, p. 102.

26. Thus the small $\Delta S = -\Delta Q$ effect suggested by our experiment cannot at present be shown to be in conflict with the limit (0.1 %) on the branching ratio for the process (4).

27. The axial current does not contribute because only currents of natural parity can be associated with the two pseudoscalar hadrons in this process.

28. Throughout our experiment, we have neglected the errors due to bremsstrahlung fluctuations in electron tracks, but this should have no significant effect on our analysis.

29. Rare decay modes of the Λ do not give rise to background, because the decay proton track is easily identified by range or ionization. We neglect the possibility of processes such as neutral $K \to \mu^+\mu^-$, which would require the existence of neutral currents.

30. For the ambiguous events, we choose the values of t^i, t^i_{min}, and t^i_{max} appropriate to the best three-body decay fit. Since the best fit may occasionally be to an incorrect decay

hypothesis, the expected errors in these quantities are larger than those for identified events. However, we find no evidence from our Monte Carlo simulation that this effect gives rise to biases in the time distribution of the ambiguous events.

31. We use the result:

$$-\delta/(\delta^2 + \tfrac{1}{4}\lambda_S^2)^{\frac{1}{2}} = \sin(43 \text{ deg}).$$

LEGAL NOTICE

This report was prepared as an account of Government sponsored work. Neither the United States, nor the Commission, nor any person acting on behalf of the Commission:

A. Makes any warranty or representation, expressed or implied, with respect to the accuracy, completeness, or usefulness of the information contained in this report, or that the use of any information, apparatus, method, or process disclosed in this report may not infringe privately owned rights; or

B. Assumes any liabilities with respect to the use of, or for damages resulting from the use of any information, apparatus, method, or process disclosed in this report.

As used in the above, "person acting on behalf of the Commission" includes any employee or contractor of the Commission, or employee of such contractor, to the extent that such employee or contractor of the Commission, or employee of such contractor prepares, disseminates, or provides access to, any information pursuant to his employment or contract with the Commission, or his employment with such contractor.

TECHNICAL INFORMATION DIVISION
LAWRENCE RADIATION LABORATORY
UNIVERSITY OF CALIFORNIA
BERKELEY, CALIFORNIA 94720